

General Disclaimer

One or more of the Following Statements may affect this Document

- This document has been reproduced from the best copy furnished by the organizational source. It is being released in the interest of making available as much information as possible.
- This document may contain data, which exceeds the sheet parameters. It was furnished in this condition by the organizational source and is the best copy available.
- This document may contain tone-on-tone or color graphs, charts and/or pictures, which have been reproduced in black and white.
- This document is paginated as submitted by the original source.
- Portions of this document are not fully legible due to the historical nature of some of the material. However, it is the best reproduction available from the original submission.

Revised

REPORT GDC-ZZL68-010
CONTRACT NAS 8-20185

**EVALUATION OF THE RADIOGRAPHIC THRESHOLD
DETECTION LEVEL OF SUBSURFACE
CRACK-LIKE DEFECTS IN ALUMINUM WELDS**

GENERAL DYNAMICS
Convair Division

FACILITY FORM 602

NGO-18895
(ACCESSION NUMBER)

5-9
(PAGES)

98355
(NASA/R OR TMX OR AD NUMBER)

1 (THRU)

32
(CODE)

(CATEGORY)

REPORT GDC-ZZL68-010

**EVALUATION OF THE RADIOGRAPHIC THRESHOLD
DETECTION LEVEL OF SUBSURFACE
CRACK-LIKE DEFECTS IN ALUMINUM WELDS**

R. W. Tryon

September 1968

Prepared Under
Contract NAS8-20185

Prepared by
CONVAIR DIVISION OF GENERAL DYNAMICS
San Diego, California

PRECEDING PAGE BLANK NOT FILMED .

FOREWORD

This report was prepared by the Convair division of General Dynamics under Technical Direction 28 issued 17 January 1968 and Technical Directive 28, Modification 1 issued 10 May 1968 on Contract NAS 8-20185. The work was administered by the Quality and Reliability Assurance Laboratory, Mechanical Methods Research Function (R-QUAL-ARM), George C. Marshall Space Flight Center, Huntsville, Alabama, with Mr. James Beal, Function Chief, Project Engineer.

The program at Convair was administered by the Reliability Control Department. Mr. K. M. Boekamp was the Convair Project Administrator and Mr. R. W. Tryon was the Convair Project Engineer.

This report covers the work performed from 24 January 1968 to 15 August 1968.

ACKNOWLEDGMENTS

The author gratefully acknowledges the assistance of his associates in the Materials Research Group and the Reliability Control Department who contributed to this study. This includes Messrs. J. F. Haskins, R. T. Anderson, and K. M. Boekamp for their technical counsel and Mr. G. Gross for conducting most of the radiographic work. Special thanks is extended to Mr. F. Jorrey who undertook the tedious task of preparing the penetrameter test blocks.

TABLE OF CONTENTS

<u>Section</u>		<u>Page</u>
1	INTRODUCTION.	1-1
2	TECHNICAL APPROACH.	2-1
3	EXPERIMENTAL PROCEDURES	3-1
	3.1 WELD TEST PLATES	3-1
	3.2 PENETRAMEETER TEST BLOCKS	3-1
	3.3 FATIGUE CRACKS	3-6
	3.4 TAPERED SLITS	3-8
	3.5 GRADUATED HOLES	3-9
	3.6 ADHESIVE BONDING	3-16
	3.7 RADIOGRAPHIC TECHNIQUE.	3-17
	3.8 RADIOGRAPHIC ANALYSTS'	3-17
	3.9 X-RAY BEAM UNIFORMITY	3-20
	3.10 ADDITIONAL RADIOGRAPHS.	3-20
4	TEST RESULTS AND DISCUSSION.	4-1
	4.1 BASELINE INFORMATION ON TEST BLOCKS.	4-1
	4.2 GRADUATED HOLE PENETRAMEETERS	4-4
	4.3 TAPER SLIT PENETRAMEETERS	4-7
	4.4 X-RAY BEAM UNIFORMITY	4-14
5	CONCLUSIONS	5-1
6	RECOMMENDATIONS.	6-1
7	REFERENCES	7-1
<u>Appendix</u>		
A	PENETRAMEETER RADIOGRAPHS.	A-1

LIST OF FIGURES

<u>Figure</u>		<u>Page</u>
1	Actual Size Radiograph of a Welded Section in Test Panel No. 6.	3-2
2	Magnified View of Radiographic Density Variation in Test Panel No. 6	3-2
3	Cross Section of 2014-T651 Aluminum Alloy Weld - Section A-A of Figure 2.	3-3
4	Magnified View of Weld B Showing Preferred Orientation of Dendrites	3-3
5	Cutting Plan for Aluminum Weld Test Panels	3-4
6	Typical Penetrameter Test Block	3-5
7	Single Edge Notched (SEN) Fatigue Specimen.	3-7
8	Fatigue Cracks Prepared in SEN Specimens	3-8
9	Fatigue Crack in 0.002-Inch-Thick Aluminum Foil Prepared for Mounting on Penetrameter Test Block	3-9
10	Types of Edge Preparation on Aluminum Foil	3-10
11	Slit-Type Penetrameter on Bottom Half of Test Block.	3-11
12	Graduated Hole Penetrameter.	3-13
13	Radiographic Test Set-up	3-18
14	Penetrameter Test Block Holder.	3-19
15	Minimum α Observed in H-5, H-4, and H-3 Penetrameters Compared to Quality Levels Required by MIL-STD-453	4-7
16	Minimum Slit Dimensions Detectable for a Fixed Radiographic Technique-Slit Parallel to X-ray Beam	4-15
17	Minimum Slit Dimensions Detectable for a Fixed Radiographic Technique-Slit 5° to X-ray Beam	4-16
18	Minimum Slit Dimensions Detectable for a Fixed Radiographic Technique-Slit 10° to X-ray Beam	4-17

LIST OF FIGURES, Contd

<u>Figure</u>		<u>Page</u>
19	Minimum Slit Dimensions Detectable for a Fixed Radiographic Technique-Slit 15° to X-ray Beam . . .	4-18
20	Minimum Slit Dimensions Detectable for a Fixed Radiographic Technique-Slit 20° to X-ray Beam . . .	4-19
21	X-ray Beam Uniformity - OEG-50 AW Tube	4-22

LIST OF TABLES

<u>Table</u>		<u>Page</u>
1	Materials and Radiographic Technique	3-6
2	Measurement of Slit Widths in Slit-Type Penetrameters.	3-12
3	Measurement of Hole Diameters in Graduated Hole Penetrameters	3-14
4	Comparison of Requested and Obtained Hole Diameters and Tolerances	3-15
5	Baseline Information on Test Blocks for Hole- Type Penetrameters	4-2
6	Baseline Information on Test Blocks for Slit- Type Penetrameters	4-3
7	Film Density Measurements of Radiographs for Hole-Type Penetrameters	4-5
8	Tabulation of Observers Versus Hole Diameters Detected in Graduated Aluminum Hole Penetrameters.	4-6
9	Film Density Measurements of Radiographs for Slit-Type Penetrameters	4-8
10	Minimum Slit Widths Detectable - X-ray Beam Parallel to Slits	4-9
11	Minimum Slit Widths Detectable - X-ray Beam Angle 5° to Slits	4-10
12	Minimum Slit Widths Detectable - X-ray Beam Angle 10° to Slits	4-11
13	Minimum Slit Widths Detectable - X-ray Beam Angle 15° to Slits	4-12
14	Minimum Slit Widths Detectable - X-ray Beam Angle 20° to Slits	4-13
15	Maximum Slit Lengths Detectable for a Fixed Radiographic Technique.	4-20
16	Summary of Slit Dimensions Detectable for a Fixed Radiographic Technique	4-21

SUMMARY

This report describes a test program whose primary objective was to design and fabricate special graduated aluminum penetrameters to evaluate the threshold detection capabilities of a fixed radiographic technique in detecting surface and subsurface cracks in one-quarter inch 2014-T651 aluminum welds. Tapered slits of predetermined dimensions were selected to simulate aligned weld cracks by bonding the penetrameters to the centerline of the weld of a matched set of weld test plates. Penetrameter thicknesses of 0.001, 0.002, 0.003, 0.004, and 0.005 in. were used to simulate crack depth. Equally thin hole-type penetrameters containing eight holes with diameters varying between $8T$ and $0.2T$ were also prepared to determine the smallest hole image resolvable under the fixed radiographic technique. Test variables evaluated included hole and slit depths between 0.001 and 0.005 in., the location of the penetrameter within the test plates, and x-ray beam angles of 0, 5, 10, 15, and 20 degrees. A total of 80 radiographs were taken, employing the same radiographic technique, equipment, and materials in all cases. The radiographic films were evaluated by five highly competent film interpreters and the threshold detection capabilities of the fixed radiographic technique were defined and compared in terms based on relationships between minimum detectable width, depth, and length of the slits and the maximum radiographic sensitivities achieved for the graduated hole penetrameters.

SECTION 1
INTRODUCTION

Aerospace requirements for high strength hardware have given added importance to the problem of flaw detection in flight vehicle structures. Of particular concern has been the demand for greater quality and reliability in critical components which have been fabricated by welding and used in cryogenic liquid propellant tankage systems. The types of flaw which are most likely to occur and exist in a critical weldment prior to service are well known. However, what is generally not known and most difficult to determine has been the size of the existing flaw, particularly when the flaw has been identified as a weld crack. It is obvious that detection of cracks combined with the determination of the crack sizes would provide quantitative data useful in fracture mechanics as an aid in evaluating and estimating the service life of critical components in cryogenic structural applications (e.g., pressure vessels, ducting).

Present methods used to predict the service life of welded tension-loaded structures include (1) proper selection of materials to meet both design and fabrication requirements, (2) application of safety factors to the design, (3) proof and leak tests, and (4) nondestructive testing. It is the latter method, nondestructive testing, in which considerable effort has been directed towards the investigation, development, or evaluation of new techniques and procedures capable of detecting as well as measuring surface and subsurface weld defects. For example, it has been recently reported that crack size can be measured in nonferrous materials by eddy current within the limitations of the technique.⁽¹⁾

One area which has received much attention by several investigators has been the meaningful correlation between various penetrameter designs, and an evaluation of those parameters which enhance or limit the ability of these technique indicators to measure in quantitative terms the radiographic sensitivity of any given radiographic technique.⁽²⁻⁶⁾ However, with the exception of the study conducted by Baker and Vannier,⁽⁶⁾ the major effort has been devoted to radiographic evaluation of materials greater than one-quarter inch in thickness.

This report discusses a test program whose primary objective has been:

To evaluate the threshold detection capabilities of a fixed radiographic technique in detecting subsurface crack-like defects in one-quarter inch 2014-T651 aluminum weldments.

SECTION 2

TECHNICAL APPROACH

Several penetrometer designs are used throughout the industry as technique indicators to measure the radiographic quality level or evaluate those parameters influencing the ability to measure radiographic sensitivity in quantitative terms. The designs are presently based upon the ability of an experienced film interpreter to resolve radiographic images produced by drilled holes, wires, tapered and parallel slits, and spheres.

Of prime interest in this program is the ability of a given radiographic technique to resolve small weld cracks and to define the detection capabilities in quantitative terms with respect to crack length, width, and depth. The closest approximation to the configuration of a naturally occurring weld crack which has been achieved to date is the taper or parallel slit technique used by several investigations to study the limitations of radiography in detecting crack-like defects. In the slit technique, cracks are simulated by placing two identical machined shims next to each other and by varying the arrangement and thickness of the shims various slit dimensions (simulating width and depth of cracks) can be obtained and the minimum detectable slit size can be determined for any given radiographic technique. The limitations of simulating the configuration of a crack with machined rectangular shims are obvious, and one important variable which cannot be reproduced by this method is the irregular shape of the edges of the crack. Another serious limitation which is peculiar to this test program is the ability to machine satisfactorily flat, square, and parallel edges on extremely thin sheet or foil.

Because of the above mentioned limitations on employing slit-type penetrameters, it was proposed that a closer approximation of a natural crack might be possibly achieved by initiating and propagating a fatigue crack in a SEN-type specimen (single-edge-notched) similar to the configuration used in fracture mechanics studies. A fatigue crack prepared in the SEN specimen, although not representative of a natural weld crack, would be a much closer approximation of a natural crack because of the irregular fractured edges and irregular crack pattern produced during propagation. This method of simulating a natural crack, therefore, was proposed as the principal technique with tapered slit technique to be used as a backup or alternate method. In both techniques, it was felt that the simulated crack dimensions (width, depth, and length) could be readily controlled or measured to obtain reliable and reproducible data regarding the minimum threshold detection level for any given radiographic technique and material thickness.

To satisfy the requirement of determining the detection capabilities of internal or subsurface weld cracks for a specific radiographic technique, a penetrometer with predetermined crack or slit dimensions (width, depth, and length) can be sandwiched between the welds of two test plates previously machined from the test material under study. Finally, by employing several of these plaque-type penetrameters, whose crack or slit dimensions are graduated and fixed in terms of width, depth, and length and sandwiching them between matched sets of welded test plates, the vanishing point of the slit or crack for each penetrometer can be determined by experienced film interpreters. Thus, with a specific set of penetrameters as described above and applied to a given material, material thickness, and radiographic technique, crack width (w) and crack depth (d) can be plotted to establish the minimum crack dimensions which are discernable under a given set of test conditions. These test data then provide a reliable and reproducible reference for either establishing or maintaining a satisfactory radiographic quality level for detecting internal crack-like weld defects. It is important to note that these special penetrameters were not to be designed to judge the type or size of weld cracks or to establish limits of acceptability.

SECTION 3

EXPERIMENTAL PROCEDURES

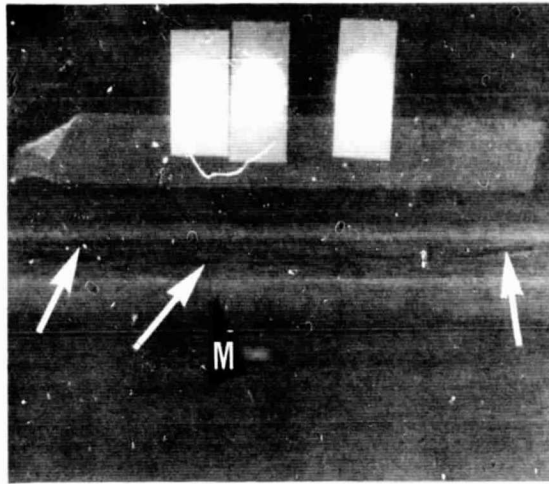
3.1 WELD TEST PLATES

Eight 2014-T651 aluminum weld panels approximately 0.3 in. x 5 in. x 33 in., submitted to Convair by MSFC to obtain the standard penetrameter test blocks, were selected for radiographic examination. Discounting weld starts and stops, the radiographs revealed only minor porosity in isolated areas; however, dark linear indications were present and found to be typical throughout most of the welds. (See Figure 1.) These radiographic indications were believed to be typical of those images produced by diffraction or reflection effects generally associated with welds exhibiting excessively large columnar grains oriented nearly parallel to the direction of radiation and identified and reported by other investigators (7,8) as "ghost line lack of fusion" or "markings." However, to verify that the indications were not associated with cracks, lack of fusion, or incomplete penetration, cross sections of the weld from each panel as well as selected areas from several panels were obtained for metallographic examination. Figure 2 shows the location of the weld cross section removed from a selected area in Panel No. 6. Although Figure 3 is cross section of the weld in Panel No. 6, it is typical of all welds metallographically examined and shows a two pass weld (one on each side) with the weld bead removed, free of the defects mentioned above, and large dendritic grains located within the central area of the last pass and oriented nearly parallel to the radiation beam. (See Figure 4.)

Four weld-test panels possessing a minimum amount of radiographic indications, distortion, and variation in bead width were selected to obtain at least twenty 1/8 in. x 2 1/2 in. x 3 1/4 in. test blocks suitable for the standard penetrameter test. The cutting plan used on all weld test panels is shown in Figure 5.

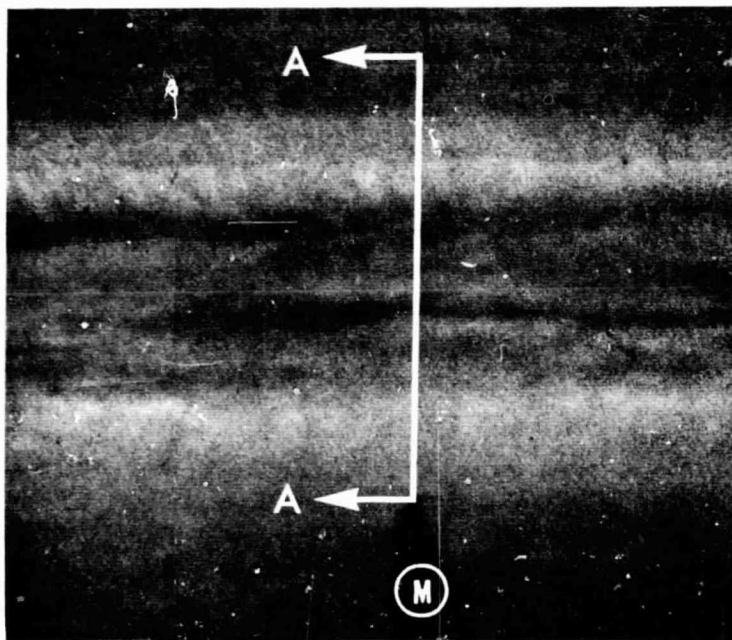
3.2 PENETRAMETER TEST BLOCKS

Following rough machining of 40 test plates, each plate was radiographed and final selection of the best 20 plates was made. Each plate was then matched and paired with respect to weld bead width, radiographic quality, and centerline of the weld, forming 10 matched sets of penetrameter test blocks, which were then finish machined (see Figure 6). Each test block was measured for thickness across the weld, x-rayed separately using the radiographic technique shown in Table 1, and the best five test blocks were selected for the slit-type penetrameters. Each plate was identified with respect to its location (top or bottom) in the test block. The test blocks for the hole-type penetrameter were identified as "H" and the test blocks for the taper slit penetrameters were identified as "C". Numbers 1 through 5 were placed after the letter to represent the thickness of the penetrameter. In all cases, the identification was metal stamped on the edge of each plate and further marked with black ink on the upper right



C4988

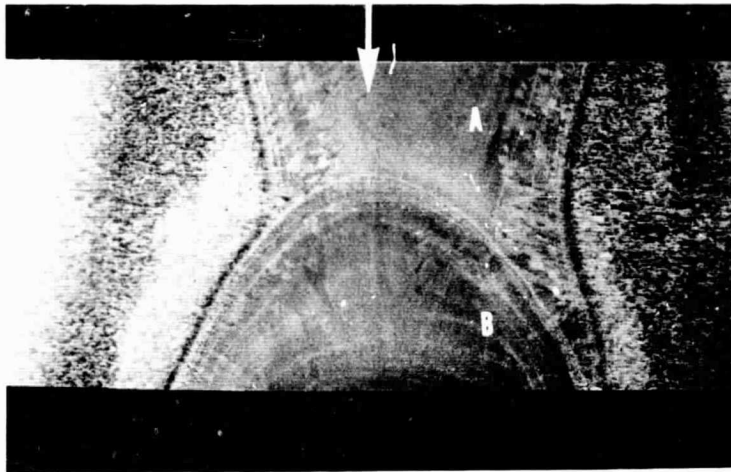
Figure 1. Actual size radiograph of a welded section in Test Panel No. 6. Arrows point to dark linear indications found to be typical in the radiographs of the 2014-T651 aluminum alloy weldments. "M" identifies location of specimens to be removed for metallographic examination. Torch travel is from left to right on the photograph.



Mag. 5X

C4989

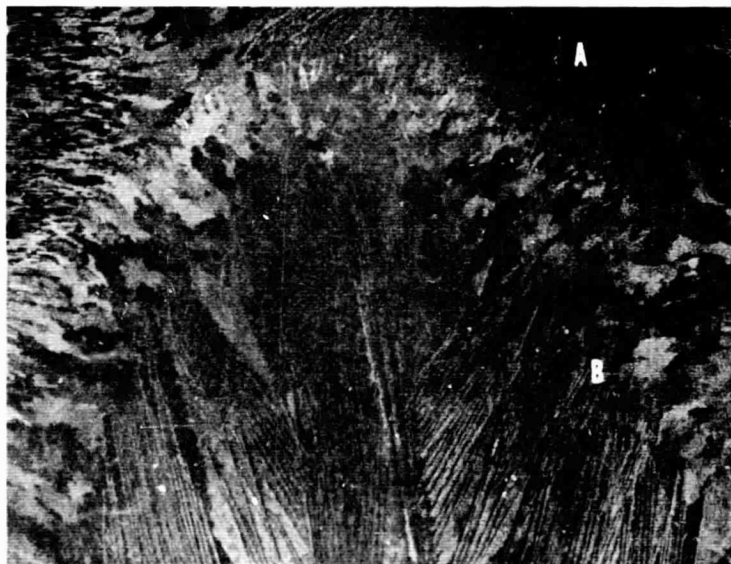
Figure 2. Magnified view of radiographic density variations within the weld area above location "M". Metallographic examination of weld conducted on sample removed through section A-A.



Mag. 6X

C4384

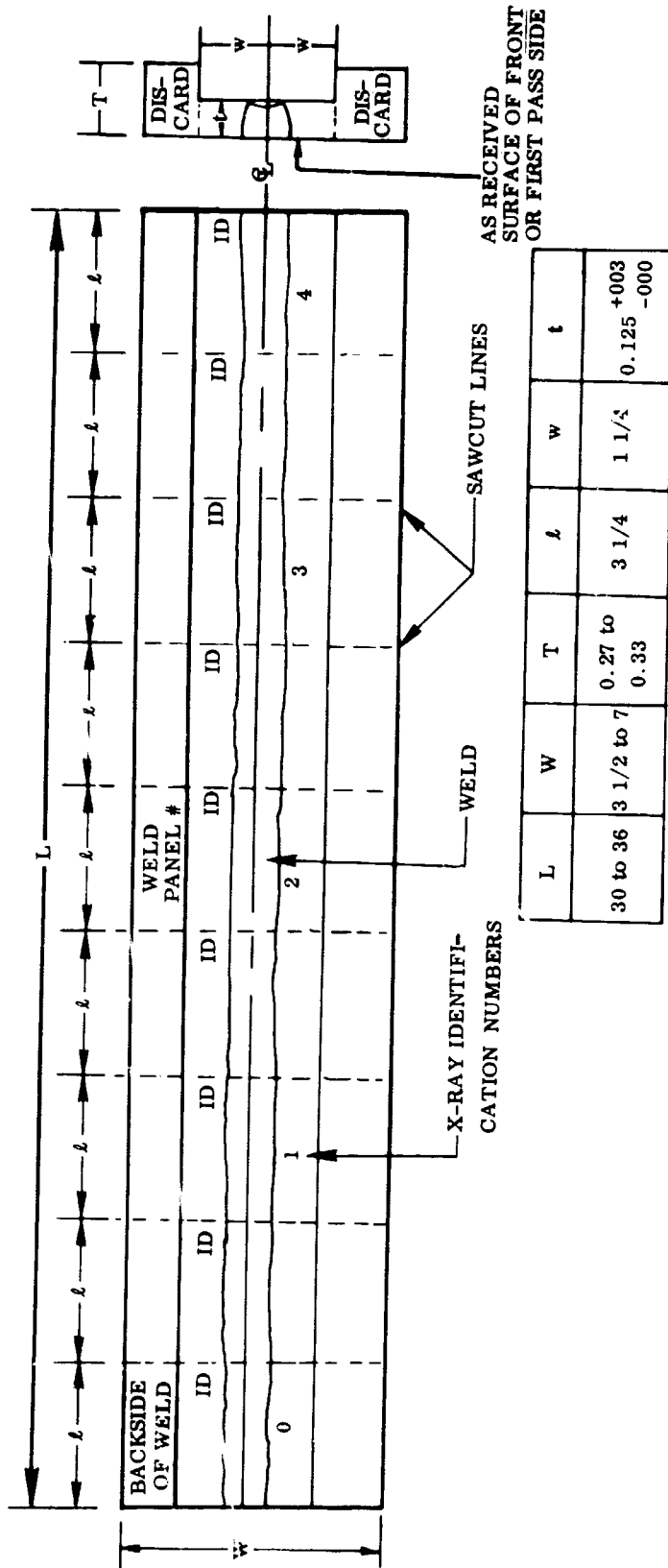
Figure 3. Cross section of 2014-T651 aluminum alloy weld at Section A-A of Figure 2. Weld is sound and free of porosity, lack of fusion, incomplete penetration, or similar defects associated with dark linear indications on radiographs. Arrow indicates direction of x-ray beam. Weld A is the first pass and weld B is the last pass (Keller's Etchant)



Mag. 15X

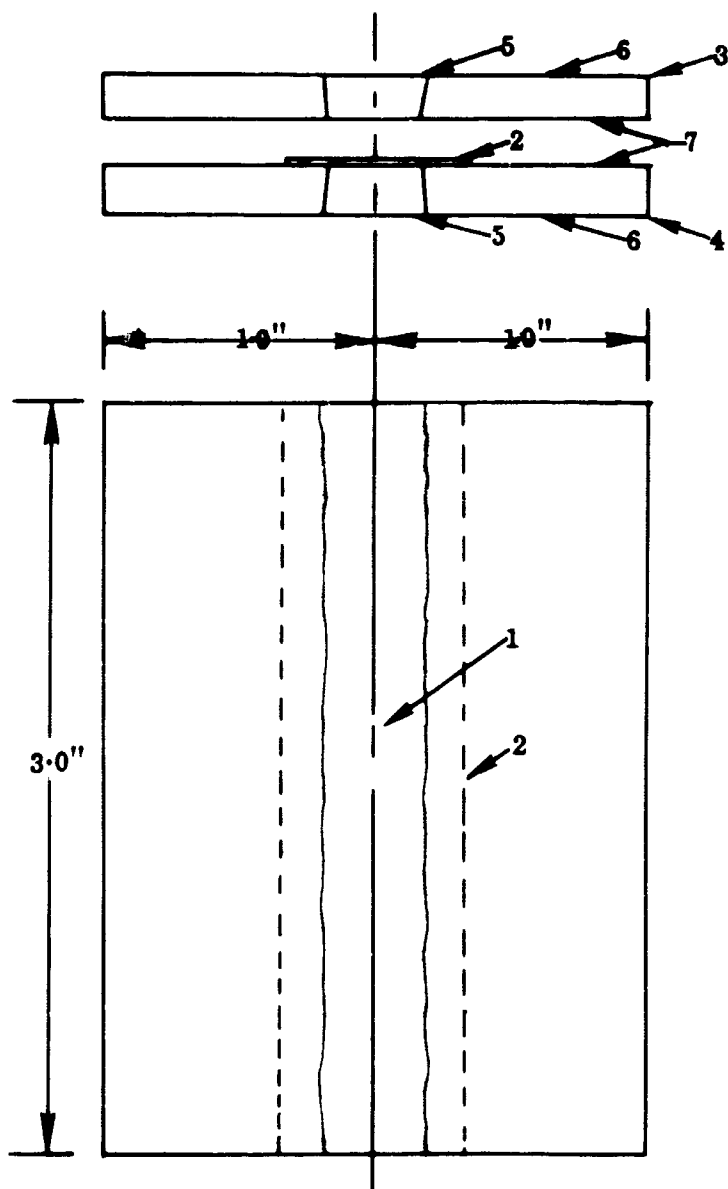
C4385

Figure 4. Magnified view of weld B showing preferred orientation of the dendrites within the central portion of the weld. A dendritic grain structure parallel or nearly parallel to the x-ray beam is believed responsible for the radiographic indications shown in Figure 1 because of the diffraction or reflection effects.



NOTE: ALL DIMENSIONS IN INCHES

Figure 5. Cutting Plan for Aluminum Weld Test Panels



1. Gas tungsten-arc weld in 2014-T651 aluminum using 4043 filler metal
2. Penetrameter bonded to bottom plate with Eastman 910 adhesive on centerline of weld.
3. Top plate (thickness = 0.125^{+003}_{-000})
4. Bottom plate (thickness = 0.125^{+003}_{-000})
5. Front or first pass side with weld bead removed to a maximum height of 0.003 in.
6. Surface not machined
7. Back or last pass side. Surface machined to final thickness dimensions on this side only to a minimum surface finish of 63 rms.

Figure 6. Typical Penetrameter Test Block

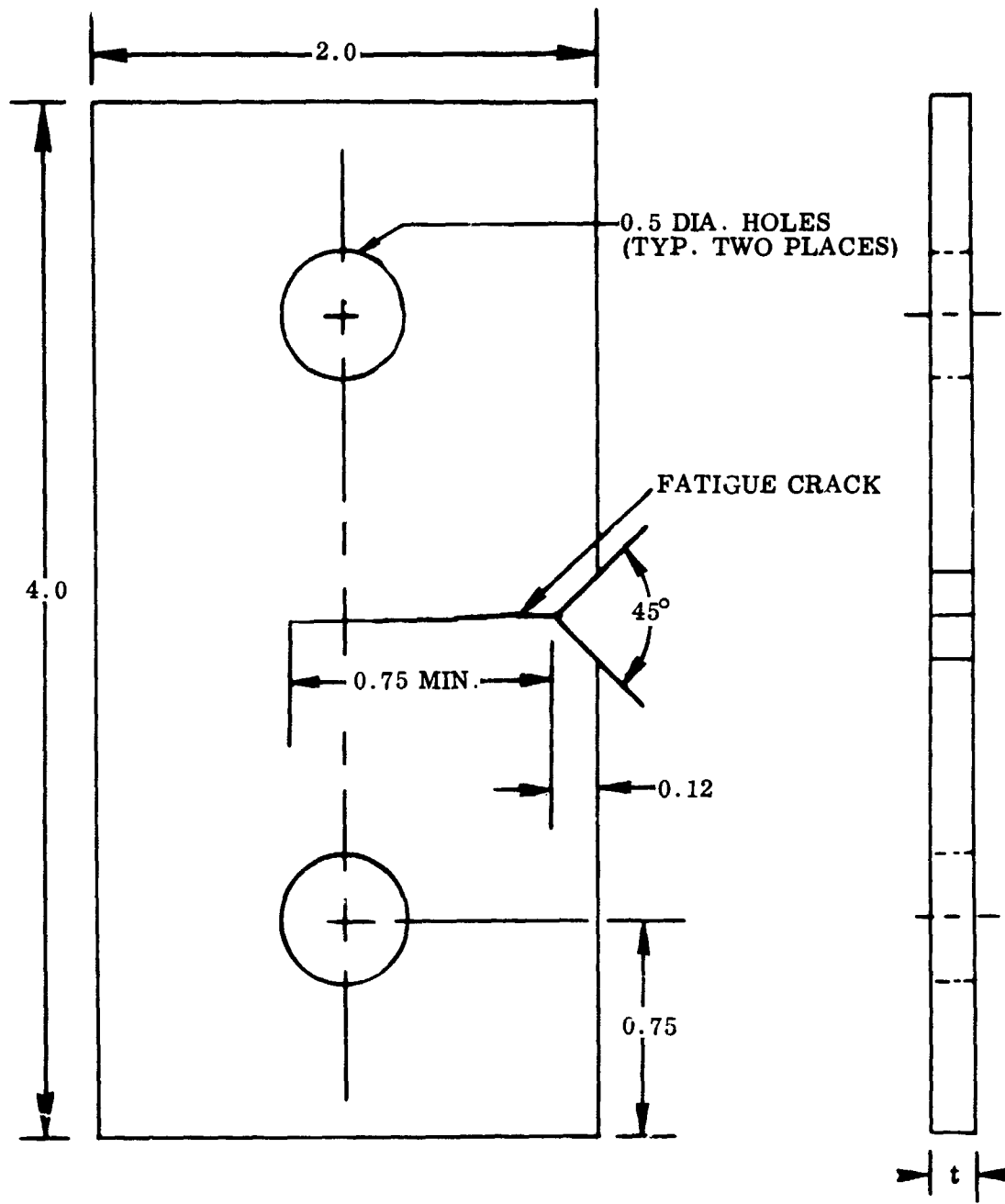
Table 1. Materials and Radiographic Technique

A. Materials	
1. Alloy	2014-T651 aluminum
2. Gage	0.251 ± 0.003 inches
3. Filler Metal	4043 aluminum wire
4. Type of Weld	inert gas tungsten-arc process; one pass both sides; weld bead removed.
B. Technique	
1. X-ray Equipment	Norelco x-ray system using a Machlett OEG-50-AW tube with a tungsten target; 50 Kv/20 ma
2. X-ray Film	Kodak Type M; 5 in. × 7 in. Ready Pack
3. Film Density	2.3 to 2.5
4. Voltage	42 Kv
5. Amperage	8 ma
6. Exposure Time	60 sec
7. Tube-Film Distance	23 in.
8. Focal Spot Size	1.5 mm
9. Processor	Eastman Kodak X-Omat
10. Densitometer	MacBeth TD 102, Quanta Log
11. Viewer	GE, Model BY, Type 1
12. Magnifier	Bell and Howell Pocket Comparator

hand corner to identify the position of the test block to be used during radiographic examination. Finally, test blocks were radiographed separately to obtain a set of reference radiographs and to evaluate the radiographic quality level of the double film technique as a method of obtaining a duplicate set of reference radiographs. Evaluation of the double film technique included the use of a standard 1/4-in. aluminum penetrometer per MIL-STD-453 placed on top and in the middle of the test blocks. In all cases, the radiographic technique shown in Table 1 was employed.

3.3 FATIGUE CRACKS

By initiating and propagating a fatigue crack in a single-edge-notched (SEN) specimen (see Figure 7), it was felt that a closer approximation to the configuration of a natural crack could be achieved, particularly with respect to the irregular shape of the

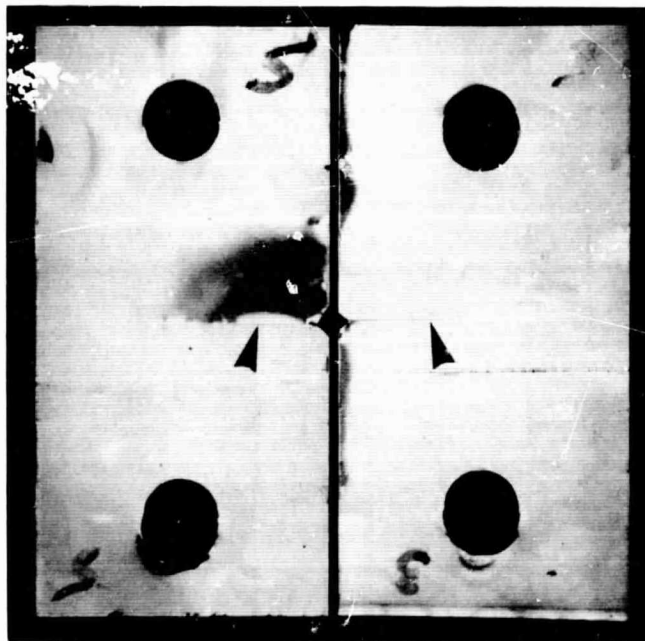


NOTE: ALL DIMENSIONS IN INCHES

t = 0.001 THRU 0.005

Figure 7. Single Edge Notched (SEN) Fatigue Specimen

fractured edges. Mechanical doublers designed to provide clamping pressure and serve as clevises were attached to the ends of a pair SEN specimens and then subjected to a low stress-high cycle condition on a SONNTAG FS-1-U Universal Fatigue Testing Machine. Fatigue cracks were produced in 0.002 in., 0.003 in., 0.004 in., and 0.005 in. aluminum foil as shown in Figure 8. Figure 9 illustrates one technique which must be used to vary the width of the crack for mounting on the test blocks. The photograph further illustrates the crimping and wrinkling which occurs as a result of handling. It was also noted that excessive handling during the fatiguing operation or preparation of a sample for bonding generally resulted in serious damage to the fractured edges. However, the major reason for discarding this method of simulating a natural crack was due to the inability to produce flat or brittle-type fatigue fractures within the capabilities of the test equipment. The fractured edges on all fatigue specimens exhibited shear-type failures typical of that shown in Figure 10B. This type of edge was not considered suitable for this test program and, therefore, was discarded in favor of the tapered slit.

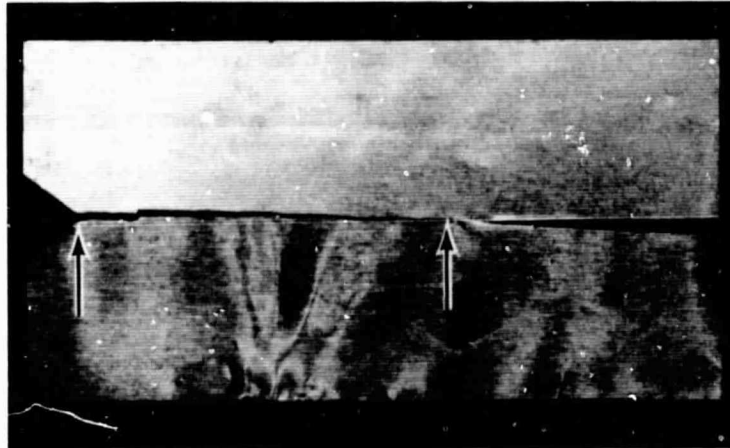


C4871

Figure 8. Fatigue cracks (arrows) prepared in SEN specimens made of 0.003 in. and 0.005 in. thick aluminum foil.

3.4 TAPERED SLITS

Five tapered slit-type penetrameters were prepared from 1100-H18 aluminum foil in thicknesses of 0.001, 0.002, 0.003, 0.004, and 0.005 inch. Foil strips of each thickness and approximately one-half inch wide and three inches long were machined with a single point diamond-capped flycutter to provide flat, square, parallel edges (see Figure 10C). The foil strips and the bottom test plate were thoroughly cleaned with solvents to remove all loose dirt and grease. The foil strips were then bonded to



Mag. 2X

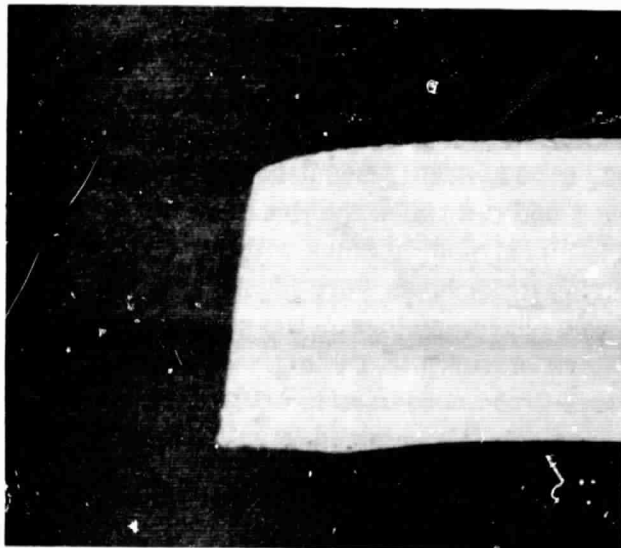
C5203

Figure 9. Fatigue crack (between arrows) in 0.002 in. thick aluminum foil prepared for mounting on penetrameter test blocks. Slit on right side of photograph was made so width of crack could be varied.

the bottom plate with Eastman 910 adhesive to form a tapered slit (see Figure 11). The width of the tapered slits varied between 0.0047 in. and 0.0067 in. at the open end and between 0.0000 in. and 0.0003 in. at the closed end. Lead marking strips were adhesively bonded to the edges of the bottom test plate and lines 1/4 in. apart were scribed into the strip with a height gauge to permanently identify the location of the slit width measurements and provide a scale for measuring slit lengths on the radiographs. The width of the slits was measured at 100X or 500X by three individuals using a metallurgical microscope and a Ramsden Filar eyepiece. This equipment was capable of measuring to the nearest 0.000020 in. The average of three readings taken at each of 12 locations for all the slit-type penetrameters is shown in Table 2.

3.5 GRADUATED HOLES

Five graduated hole-type penetrameters were prepared from 1100-H38 aluminum foil in thicknesses of 0.001, 0.002, 0.003, 0.004, and 0.005 inch as shown in Figure 12. Hole diameters varied between 8 and 0.2 times the thickness of the penetrameter and were microdrilled⁽⁹⁾ to provide cleanly-bored holes within the required tolerances. Cleaning, bonding, and measuring procedures were identical to those procedures used in the preparation of the slit-type penetrameters. The measurement of hole diameters in all the hole-type penetrameters is shown in Table 3. In addition, Table 4 was prepared to compare the differences in the penetrameter hole diameters and tolerances as originally requested with those actually obtained by microdrilling.



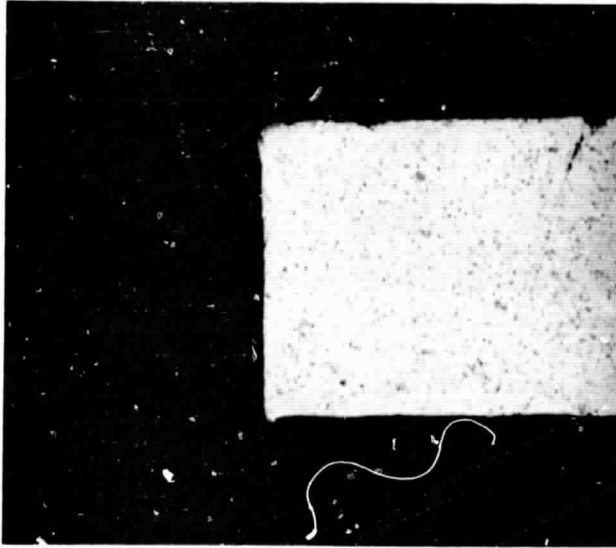
C4417

A. Slitter
(angle = 7°)



C4418

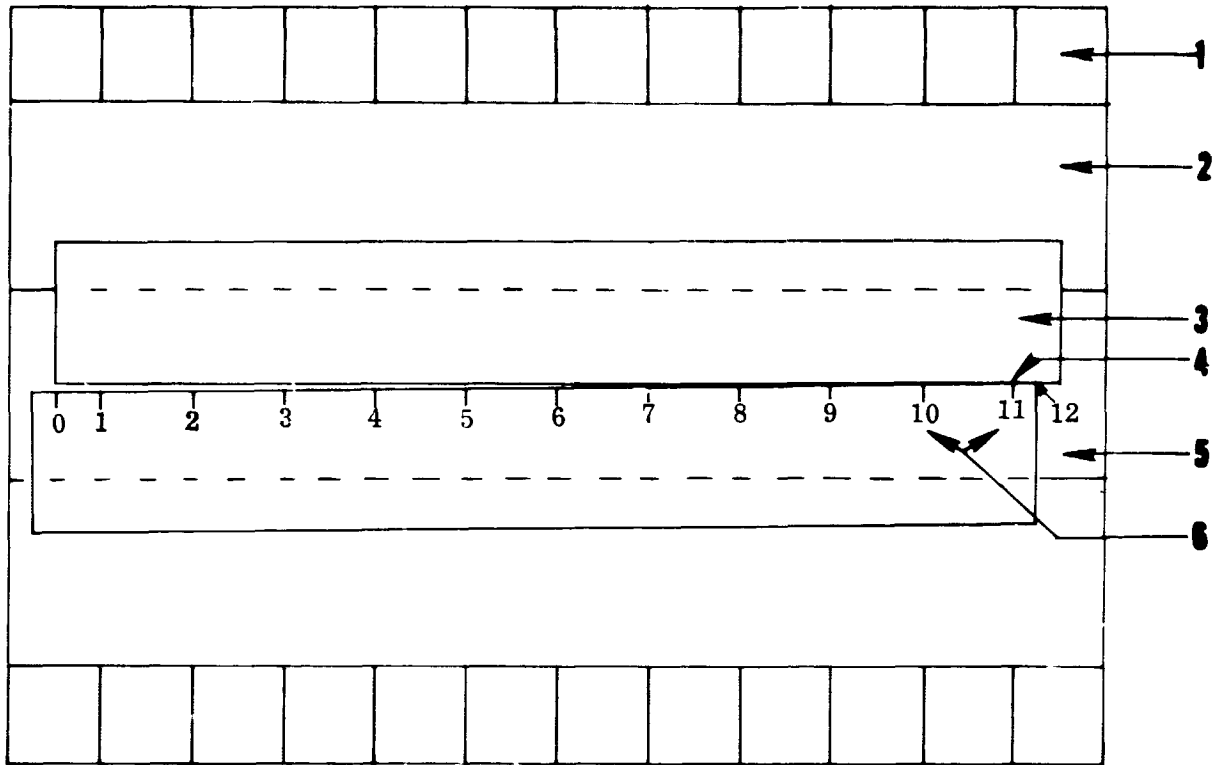
B. Fatigue Fracture
(angle = 40°)



C4974

C. Flycutter
(angle < 1°)

Figure 10. Types of edge preparation on aluminum foil (magnification 500 X; unetched). The edges prepared by Method C were used for slit-type penetrameters.



- 1** Lead marker with lines equally spaced 1/4 in. apart
- 2** Bottom half of penetrometer test block
- 3** Aluminum foil 0.001 in. thru 0.005 in. thick bonded to block with Eastman 910 adhesive to form slit.
- 4** Slit with edges machined square and flat.
- 5** Weld
- 6** Numbers indicate the location of slit width measurements and, with the exception of locations 0 and 12, are aligned with the lead markers.

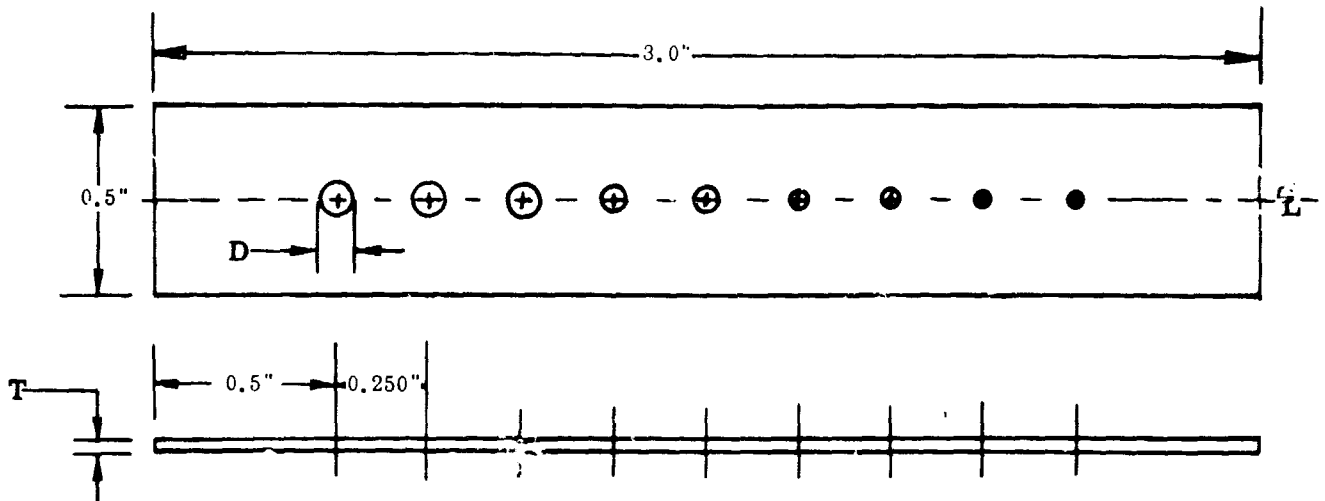
Figure 11. Slit-type Penetrometer on Bottom Half of Test Block

Table 2. Measurement of Slit Widths in Slit-type Penetrators⁽¹⁾

I. D.	Penetrator Thickness (mils)	Slit Width in Mils at Location ⁽²⁾												
		0	1	2	3	4	5	6	7	8	9	10	11	12
C-5	5	5.8	5.5	4.7	4.4	3.8	3.3	3.0	2.4	2.1	1.4	0.9	0.4	0.2
C-4	4	6.3	5.8	5.2	4.5	3.9	3.2	2.8	2.1	1.6	1.2	0.9	0.6	0.3
C-3	3	4.7	4.2	3.7	3.1	2.7	2.4	2.0	1.7	1.4	1.1	0.9	0.6	0.3
C-2	2	5.6	5.4	5.0	4.3	3.9	3.5	3.0	2.6	2.3	1.7	1.3	0.5	0.2
C-1	1	6.7	6.6	6.2	5.7	5.1	4.4	3.8	3.2	2.4	1.6	0.9	0.2	0.0

(1) All values represent the average of three readings taken at each location by three different observers using the same measuring equipment.

(2) "0" location is at the open end of the slit while location 12 is at the closed end of the slit. Location numbers 1 thru 11 are equally spaced 1/4 in. apart, e.g., measured from the edge of the test block, location number 4 equals a length of 1 in. and location number 9 equals a length of 2 1/4.



T, Mils	D in Mils For Hole								
	1	2	3	4	5	6	7	8	9
5	40	20	10	5	4	3	2	1.5	1.0
4	32	16	8	4	3.2	2.4	1.6	1.2	-
3	24	12	6	3	2.4	1.8	1.2	0.9	-
2	16	8	4	2	1.6	1.2	0.8	0.6	-
1	8	4	2	1	0.8	0.6	0.4	0.3	-

NOTES:

1. Holes shall be equally spaced 0.250 ± 0.010 in. and shall be drilled true and normal to the surface.
2. Holes shall not be recessed or chamfered and shall be clean and free of burrs.
3. Hole diameter tolerances shall be as follows:
 - a. 0.040 in. thru 0.004 in. - plus or minus 5%
 - b. 0.003 in. thru 0.001 in. - plus or minus 10%
 - c. less than 0.001 in. - close as practical.
4. Diameter (D) of holes 1 thru 9 to be equivalent to 8T, 4T, 2T, 1T, 0.8T, 0.6T, 0.4T, 0.3T, and 0.2T, respectively, where T equals penetrometer thickness.
5. Material shall be 1190-H18 aluminum alloy foil.

Figure 12. Graduated Hole Penetrameters

Table 3. Measurement of Hole Diameters in Graduated Hole Penetrater

Penetrater		Hole Diameter, mils ⁽¹⁾⁽²⁾									
I. D.	Thickness (mils)	8T	4T	2T	1T	0.8T	0.6T	0.4T	0.3T	0.2T	
H-5	5	40.7	20.6	10.3	5.4	4.3	3.1	2.0	1.5	1.1	
H-4	4	32.8	16.5	8.1	4.3	3.6	2.5	1.7	1.5	(3)	
H-3	3	24.9	12.6	6.2	3.1	2.7	2.1	1.2	1.0	(3)	
H-2	2	16.2	8.0	4.1	2.0	1.7	1.2	0.8	0.6	(3)	
H-1	1	8.1	4.1	2.1	1.1	0.8	0.7	0.6	0.4	(3)	

(1) All values represent the average of three readings obtained by three different observers using the same measuring equipment.
(2) Tolerance on all hole diameters is 0.1 mil.
(3) Thickness of penetrater prevents drilling holes smaller than 0.3T.

Table 4. Comparison of Requested and Obtained Penetrameter Hole Diameters and Tolerances

Number of Holes	Hole Dimensions Requested (inch)	Hole Dimensions Obtained (inch)	Remarks ^(d)
1	0.040 ±0.0020	0.0407 ±0.0001	OK
1	0.032 ±0.0016	0.0328 ±0.0001	OK
1	0.024 ±0.0012	0.0249 ±0.0001	OK
1	0.020 ±0.0010	0.0206 ±0.0001	OK
2	0.016 ±0.0009	0.0165 ±0.0001	OK
		0.0162 ±0.0001	OK
1	0.012 ±0.0006	0.0125 ±0.0001	0.0001 O/S
1	0.010 ±0.0005	0.0103 ±0.0001	OK
3	0.008 ±0.0004	0.0081 ±0.0001	OK
		0.0080 ±0.0001	OK
		0.0081 ±0.0001	OK
1	0.006 ±0.0003	0.0062 ±0.0001	OK
1	0.005 ±0.0002	0.0054 ±0.0001	0.0003 O/S
4	0.004 ±0.0002	0.0043 ±0.0001	0.0002 O/S
		0.0043 ±0.0001	0.0002 O/S
		0.0041 ±0.0001	OK
		0.0041 ±0.0001	OK
1	0.0032 ±0.0003	0.0036 ±0.0001 ^(b)	0.0002 O/S
2	0.0030 ±0.0003	0.0031 ±0.0001	OK
		0.0031 ±0.0001	OK
2	0.0024 ±0.0002	0.0025 ±0.0001	OK
		0.0027 ±0.0001	0.0002 O/S
3	0.0020 ±0.0002	0.0020 ±0.0001	OK
		0.0020 ±0.0001	OK
		0.0021 ±0.0001	OK
1	0.0018 ±0.0002	0.0021 ±0.0001 ^{(b)(c)}	0.0002 O/S
2	0.0016 ±0.0002	0.0017 ±0.0001	OK
		0.0017 ±0.0001	OK
1	0.0015 ±0.0002	0.0015 ±0.0001	OK
3	0.0012 ±0.0001	0.0012 ±0.0001	OK
		0.0012 ±0.0001	OK
		0.0015 ±0.0001 ^{(b)(c)}	0.0003 O/S
2	0.0010 ±0.0001	0.0011 ±0.0001 ^(b)	0.0001 O/S
		0.0011 ±0.0001 ^(b)	0.0001 O/S
1	0.0009 ±0.0001 ^(a)	0.0010 ±0.0001 ^(b)	0.0001 O/S
2	0.0008 ±0.0001 ^(a)	0.0008 ±0.0001	OK
		0.0008 ±0.0001	OK

Table 4. Comparison of Requested and Obtained Penetrameter Hole Diameters and Tolerances (Continued)

Number of Holes	Hole Dimensions Requested (inch)	Hole Dimensions Obtained (inch)	Remarks (d)
2	0.0006 ± 0.0001 (a)	0.0006 ± 0.0001	OK
1	0.0004 ± 0.0001 (a)	0.0007 ± 0.0001	0.0001 O/S
1	0.0003 ± 0.0001 (a)	0.0006 ± 0.0001 (b)(c)	0.0002 O/S
		0.0004 ± 0.0001	0.0001 O/S

(a) Tolerance for holes less than 0.001 inch estimated at 0.0001 inch.
 (b) Next lower drill size needed to bring hole diameters within specified dimensions.
 (c) Obvious improper drill size used.
 (d) 66% of all holes drilled were to print requirements.
 Oversized (O/S) holes occurred most frequently on hole diameters $\bar{<}$ 0.005 inch.

3.6 ADHESIVE BONDING

All penetrameters were bonded to the bottom test plate with Eastman 910 adhesive to prevent damage or distortion during subsequent handling. More important, however, bonding fixed the location of the penetrameter within the weld area and fixed the dimensions of the tapered slits, thus providing a high degree of assurance that the test data on these penetrameters, when evaluated under similar test conditions, are readily reproducible.

Eastman 910 adhesive was used for bonding because of its rapidity to form a strong aluminum-aluminum bond without the use of heat, catalysts, solvents, or excessive pressure. The penetrameters and bottom plates were thoroughly cleaned with methyl ethyl ketone to remove all loose dirt, chips, and grease. Approximately one drop of Eastman 910 was applied to one side of the penetrameter strip then spread over the surface with a dissecting needle. Care was exercised to prevent the adhesive from flowing to the edges of the taper slit or into the penetrameter holes. Light pressure was applied for approximately 2 minutes and the adhesive allowed to cure at room temperature for 48 hours to develop maximum bond strength. All measurements of hole diameters and widths of the tapered slits were made after bonding. The penetrameters can be readily removed from the test plates without damage by soaking the plates in an undiluted solution of N, N-dimethylformamide at room temperature for a period of 48 to 96 hours. The lead marking strips are pressure sensitive tapes and can readily be removed without damage to the bottom test plates.

3.7 RADIOGRAPHIC TECHNIQUE

Each penetrameter test block was radiographed separately employing the same radiographic materials, equipment and technique described in Table 1. A typical radiographic test set-up is shown in Figure 13. Each test block was also radiographed under all test variables at a fixed position under the geometric centerline of the x-ray beam by using an aluminum penetrameter test block holder fabricated to the dimensions shown in Figure 14.

For the hole-type penetrameters, the test variables were limited to a radiation beam angle normal to the test block and to two penetrameter locations (top and middle). Thus, 10 radiographs were needed to evaluate the fixed radiographic technique using hole-type penetrameters; i. e., 1 x-ray beam angle \times 2 penetrameter locations \times 5 penetrameter thicknesses.

For the taper slit penetrameters, the test variables included radiation beam angles of 0, 5, 10, 15, and 20 degrees and the two penetrameter locations (top or middle) for each beam angle. Thus, 50 radiographs were needed to evaluate these variables and determine the minimum detectable slit dimensions for the fixed radiographic technique; i. e., 5 x-ray beam angles \times 2 penetrameter locations \times 5 penetrameter thicknesses.

It should be pointed out that, in addition to the fixed radiographic materials, equipment, and technique described in Table 1 and employed in this test program to obtain and evaluate all radiographs, the following test restraints were also imposed:

- a. Measuring equipment and personnel acquainted with the use of this equipment.
- b. Fixed penetrameter location within the weld area and under the x-ray beam.
- c. Fixed tapered slit dimensions and hole diameters.
- d. Film evaluation at a density range between 2.3 and 2.5.
- e. Personnel highly experienced in film interpretation.

3.8 RADIOGRAPHIC ANALYSTS

All radiographs made during the course of this test program were interpreted by at least five highly qualified analysts, each possessing an extensive background in all phases of industrial radiography. Three of the five analysts selected for this study are permanently assigned to the x-ray laboratories of the Reliability Control Department and are responsible for the radiographic inspection of critical aerospace or aircraft components and structures currently in production. Furthermore, four of five analysts are technically qualified to train other individuals in current theory and application of industrial radiography and have been assigned as instructors in Convair's Nondestructive Training Program.

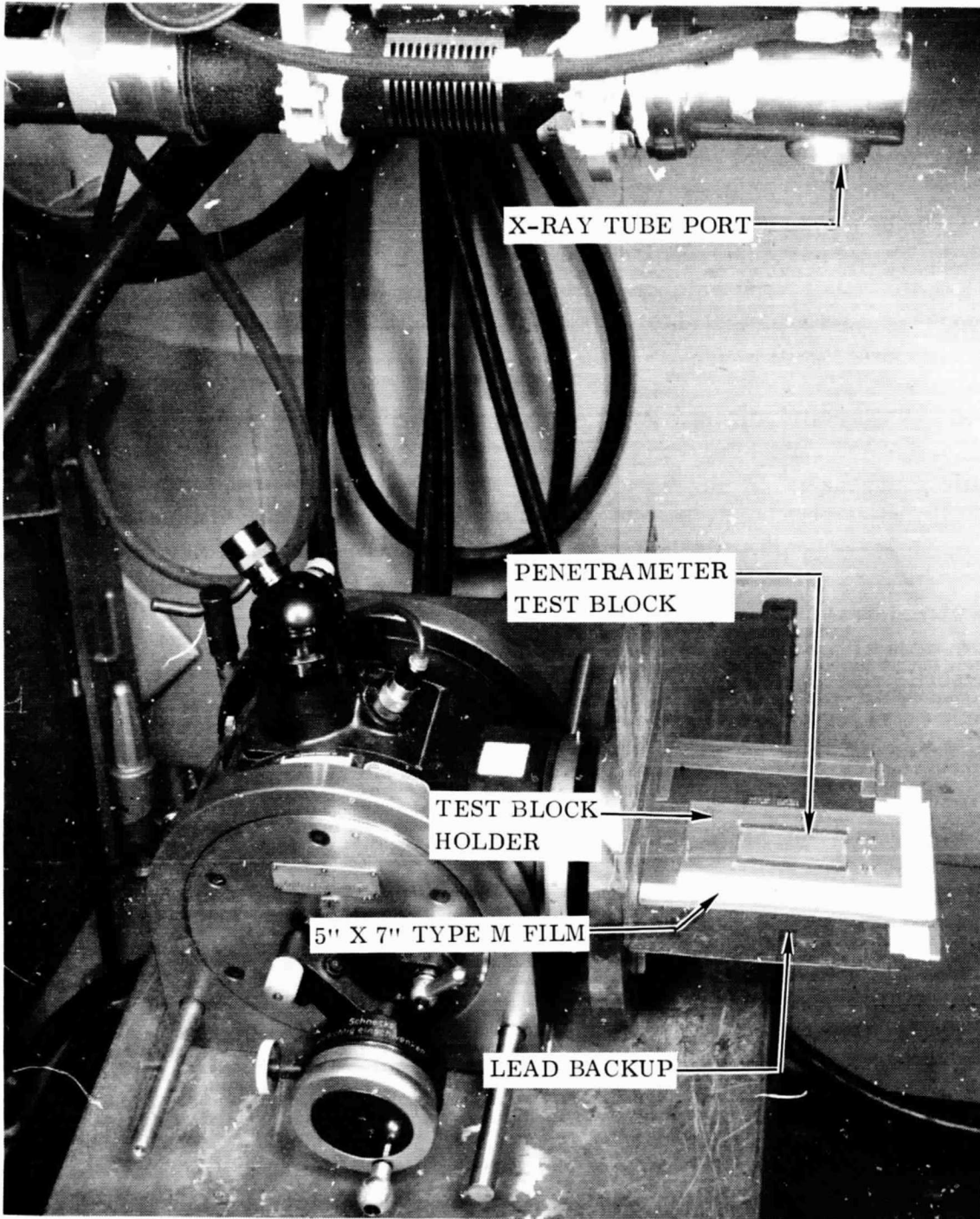
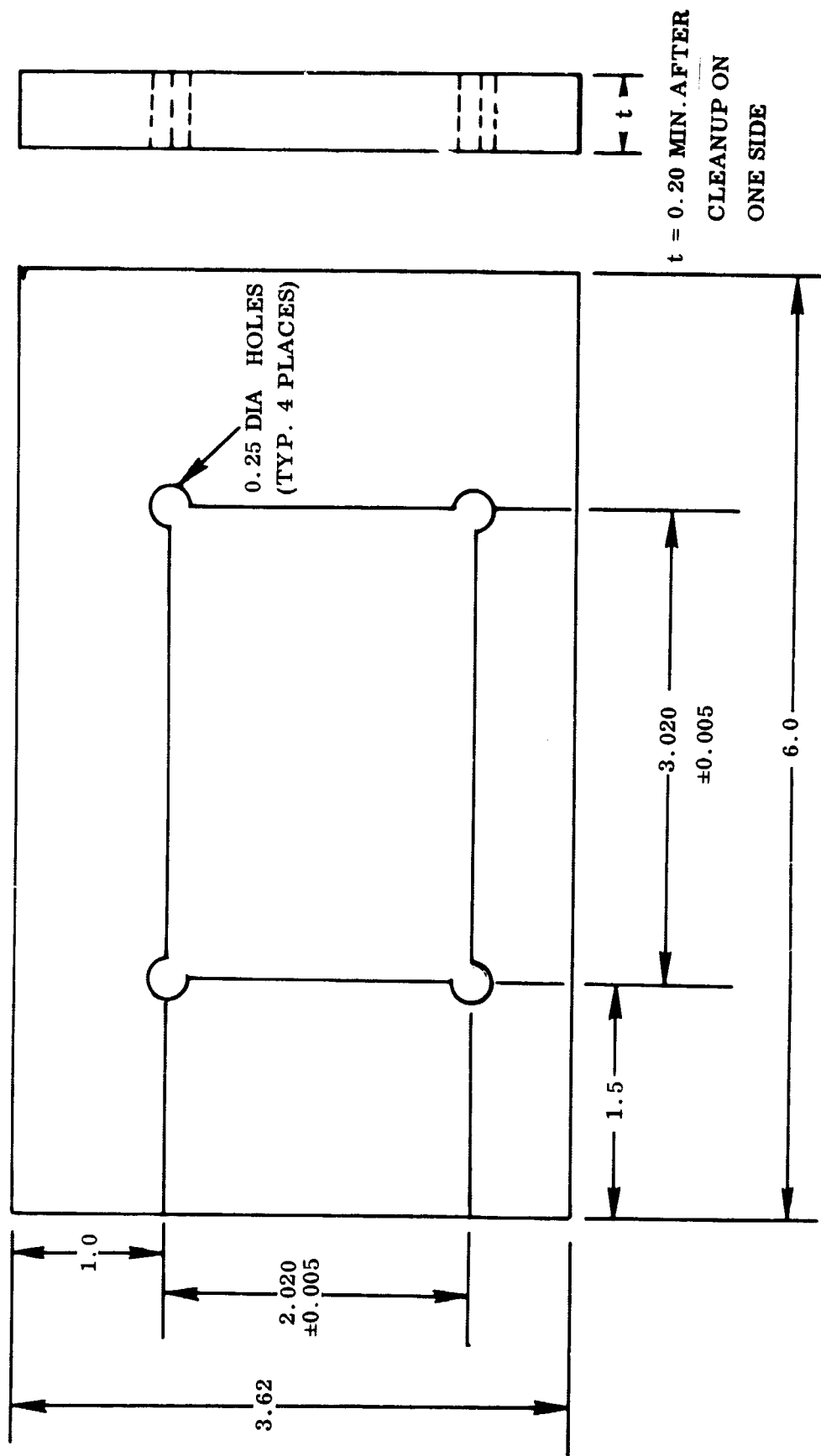


Figure 13. Radiographic Test Setup



NOTE: ALL DIMENSIONS IN INCHES

Figure 14. Penetrameter Test Block Holder

3.9 X-RAY BEAM UNIFORMITY

At the completion of all tests, a contour map of the diffuse transmission density within the penetrometer test block area was prepared to evaluate and describe the uniformity of the x-ray beam. The test conditions used to perform this test were identical to those radiographic materials, equipment, and technique employed in this test program except that the film was processed by hand.

3.10 ADDITIONAL RADIOGRAPHS

An additional 12 radiographs were supplied to MFSC to evaluate a technique capable of detecting hole or slit dimensions considerably below those dimensions ordinarily resolvable by visual means. The 2 and 4 mil thicknesses of both the hole and taper slit penetrometers were radiographed individually to obtain one set of radiographs with a density range of 2.3 to 2.7 and another set of radiographs with a density range of 1.1 to 1.2. All radiographs were taken at a fixed location normal to the geometric centerline of the x-ray beam to avoid angulation effects. Radiographs with a density range of 2.3 to 2.7 were obtained using the same radiographic technique and equipment as described in Table 1. To obtain radiographs with a density range of 1.1 to 1.2, voltage and amperage had to be reduced to 36 Kv and 5 ma, respectively, while all other parameters were held constant.

SECTION 4

TEST RESULTS AND DISCUSSION

4.1 BASELINE INFORMATION ON TEST BLOCKS

Prior to bonding the penetrameters to the bottom plate, each matched set of test blocks was radiographed separately using the double film technique and the fixed radiographic parameters for the following reasons:

- a. To provide a basis of comparing the dark linear indications found within the weld area with similar features on subsequent radiographs.
- b. To determine the radiographic sensitivity for the fixed radiographic technique using the standard penetrometer for 1/4-inch aluminum per MIL-STD-453 placed outside the weld area and on the top or the middle of the test blocks.
- c. To compare density values and evaluate the application of obtaining a duplicate set of penetrometer radiographs for film evaluation.

The test data obtained for baseline information on all test blocks are presented in Tables 5 and 6. The baseline radiographs for both the hole-type and slit-type penetrometer test blocks can be found in the Appendix on pages A-2 through A-11.

The test results show that the required minimum radiographic quality level of 2-2T was attained under most of the conditions investigated with the double film technique. However, there were five instances where the resolution of the hole images was reduced to a 2-4T level and in four of these five cases it occurred on the back film and when the penetrometer was located at the middle of the test block. It is obvious that such noted differences in radiographic sensitivity between the front and back films would result in considerable variation in test data because the hole and slit images produced on the back film would not be an exact duplicate of those same images produced on the front film. For this reason, therefore, the double film technique was not considered to be a suitable means of producing a duplicate set of standard radiographs for final evaluation.

The test results also show that the film densities varied between 2.19 and 2.40 for the front film and between 2.12 and 2.39 for the back film. Furthermore, it was noted that the average difference in density values between the front and back film was as large as 0.20, whereas the difference in density values with respect to penetrometer location (top or middle) did not exceed 0.05. It is apparent from the test results, however, that these density variations were not significant factors in achieving a radiographic quality level of 2-2T.

Table 5. Baseline Information on Test Blocks for Hole-Type Penetrameters

Block Number	Thickness (inches)	Film Location ⁽¹⁾	Penetrameter Location ⁽²⁾⁽⁴⁾	Film Density ⁽³⁾	Min. Perceptible Penetrameter Hole
H-1	0.254	Front	T	2.34	2T
			M	2.31	2T
		Back	T	2.20	2T
			M	2.18	2T
H-2	0.248	Front	T	2.32	2T
			M	2.35	2T
		Back	T	2.20	2T
			M	2.24	4T
H-3	0.251	Front	T	2.38	2T
			M	2.40	2T
		Back	T	2.39	2T
			M	2.38	4T
H-4	0.251	Front	T	2.25	2T
			M	2.19	2T
		Back	T	2.18	2T
			M	2.12	2T
H-5	0.251	Front	T	2.40	2T
			M	2.34	2T
		Back	T	2.20	2T
			M	2.12	2T

(1) Double film technique. "Front" refers to film closest to x-ray tube.

(2) Penetrameter per MIL-STD-453 for 1/4 in. aluminum placed outside of the weld area either on top of test block (top) or sandwiched between the two 1/8 in. x 2 in. x 3 in. plates (middle) which comprise the test block.

(3) Average of three readings

(4) T = Top
M = Middle

Table 6. Baseline Information on Test Blocks for Slit-Type Penetrameters

Block Number	Thickness (inches)	Film Location ⁽¹⁾	Penetrameter Location ⁽²⁾⁽⁴⁾	Film Density ⁽³⁾	Min. Perceptible Penetrameter Hole
C-1	0.248	Front	T	2.38	2T
			M	2.30	2T
		Back	T	2.34	2T
			M	2.28	4T
C-2	0.250	Front	T	2.36	2T
			M	2.32	2T
		Back	T	2.28	2T
			M	2.24	4T
C-3	0.251	Front	T	2.36	2T
			M	2.33	2T
		Back	T	2.17	2T
			M	2.12	2T
C-4	0.249	Front	T	2.24	4T
			M	2.22	2T
		Back	T	2.14	2T
			M	2.20	2T
C-5	0.248	Front	T	2.30	2T
			M	2.38	2T
		Back	T	2.14	2T
			M	2.18	2T

(1) Double film technique. "Front" refers to film closest to x-ray tube.

(2) Penetrameter per MIL-STD-453 for 1/4 in. aluminum placed outside of the weld area either on top of test block (top) or sandwiched between the two 1/8 in. x 2 in. x 3 in. plates (middle) which comprise the test block.

(3) Average of three readings

(4) T = Top
M = Middle

An examination of the reference radiographs made on the test blocks and shown in the Appendix on pages A-2 through A-11 clearly illustrates that all welds are free of the common defects such as cracks, porosity, lack of fusion, and incomplete penetration. However, dark linear indications attributable to the diffraction or reflection effects of the dendritic grain structure within the weld are still present, but they are less well-defined and not as prominent when compared to similar indications previously encountered during the radiographic inspection of the weld test plates (see Figure 1). Significantly, the indications which are present on these reference radiographs are for the most part outside the critical area, i.e., the central portion of the weld, thus minimizing the chance that their presence would interfere with an analyst's ability to resolve small hole images or detect the vanishing point of the slits on subsequent radiographs. It should be pointed out that the indications on the baseline radiographs are predictable and reproducible with respect to appearance and location only when the machined surfaces of the top and bottom plate are in contact with each other and the test block is normal to the x-ray beam. This position can be compared to the penetrometer test blocks placed at a zero degree angle to the x-ray beam with the penetrometer sandwiched between the top and bottom plates. As would be expected, the appearance, location, and other characteristics of these dark linear indications for all other positions changes as a function of the beam angle and/or the location of the penetrometer. It was noted on subsequent radiographs that when the top and bottom plates of the test block were interchanged, i.e., penetrometer located on top of the test block, the dark linear indications completely disappeared or their number was significantly reduced. The reason for this effect can be attributed to the disregister of the dendritic grain structure.

4.2 GRADUATED HOLE PENETRIMETERS

The radiographs taken on the five graduated hole penetrimeters placed normal to the x-ray beam are shown in pages A-12 through A-16 in the Appendix. The film density measurements obtained on each radiograph are shown in Table 7; each value represents the average of three readings taken on the upper part of the test block between the penetrimeter and the lead marking strip. Film density values ranged from 2.33 to 2.46 and indicated that no correlation exists between density and penetrimeter location.

A summary of the hole diameters detected in all graduated hole penetrimeters by six observers is shown in Table 8 and is self-explanatory. In general, however, the results show that the average observer was not capable of resolving hole images in penetrimeter thicknesses less than 0.003 in. even though the outline of the penetrimeter was visible to all observers down to 0.002 in. thickness. All observers were capable of detecting at least a 4T hole in the H-5 and H-4 penetrimeters regardless of location within the test block. With the exception of one observer, the 1T hole was not resolvable in any penetrimeter including H-5 as would be expected considering the radiographic technique which was employed.

**Table 7. Film Density Measurements of Radiographs
for Hole-Type Penetrators**

Penetrator Identification	Penetrator Location ⁽²⁾	Film Density ⁽¹⁾
H-1	T	2.46
	M	2.43
H-2	T	2.37
	M	2.42
H-3	T	2.36
	M	2.38
H-4	T	2.42
	M	2.39
H-5	T	2.34
	M	2.33

(1) Average of three readings taken on the upper part of the plate between the penetrator and Pb marking strip.
(2) T = Top
M = Middle

When the minimum detectable hole dimensions as resolved by the average observer are converted and expressed as an alpha value then plotted as a function of thickness as shown in Figure 15, the results show that a radiographic quality level of 2-2T or better was achieved for this technique in three out of six instances and did not exceed a 2-4T level for all minimum alphas observed. These test results also indicate that a 2-2T quality level was more readily obtained when the penetrator was sandwiched between the test plates. As shown in Table 8, the 2T hole in the H-5 penetrator which represents the MIL-STD-453 penetrator used for 1/4-in. aluminum was detectable 100 percent of the time when placed in the weld area and between the test plates. It should be pointed out, however, that the 2T hole in the standard penetrator of similar thickness was detectable by all observers for this fixed radiographic technique when the penetrator was located outside of the weld area and placed either on the top or in the middle of the test blocks (see Table 5).

Table 8. Tabulation of Observers versus Hole Diameter Detected in Graduated Aluminum Hole Penetrators

Penetrator I.D. Thickness (mils)	Top										Center								
	Hole Number						Hole Number												
	8T	4T	2T	1T	0.8T	0.6T	0.4T	0.3T	0.2T	8T	4T	2T	1T	0.8T	0.6T	0.4T	0.3T	0.2T	
H-5	6	6	2	1															
H-4	6	6	5	1															
H-3	5	2	1																
H-2	2	1																	
H-1	1																		

NOTES:

1. Total number of observers was six.
2. Outline of H-2 penetrator readily visible to all observers.
3. All penetrators located on the weld and normal to x-ray beam

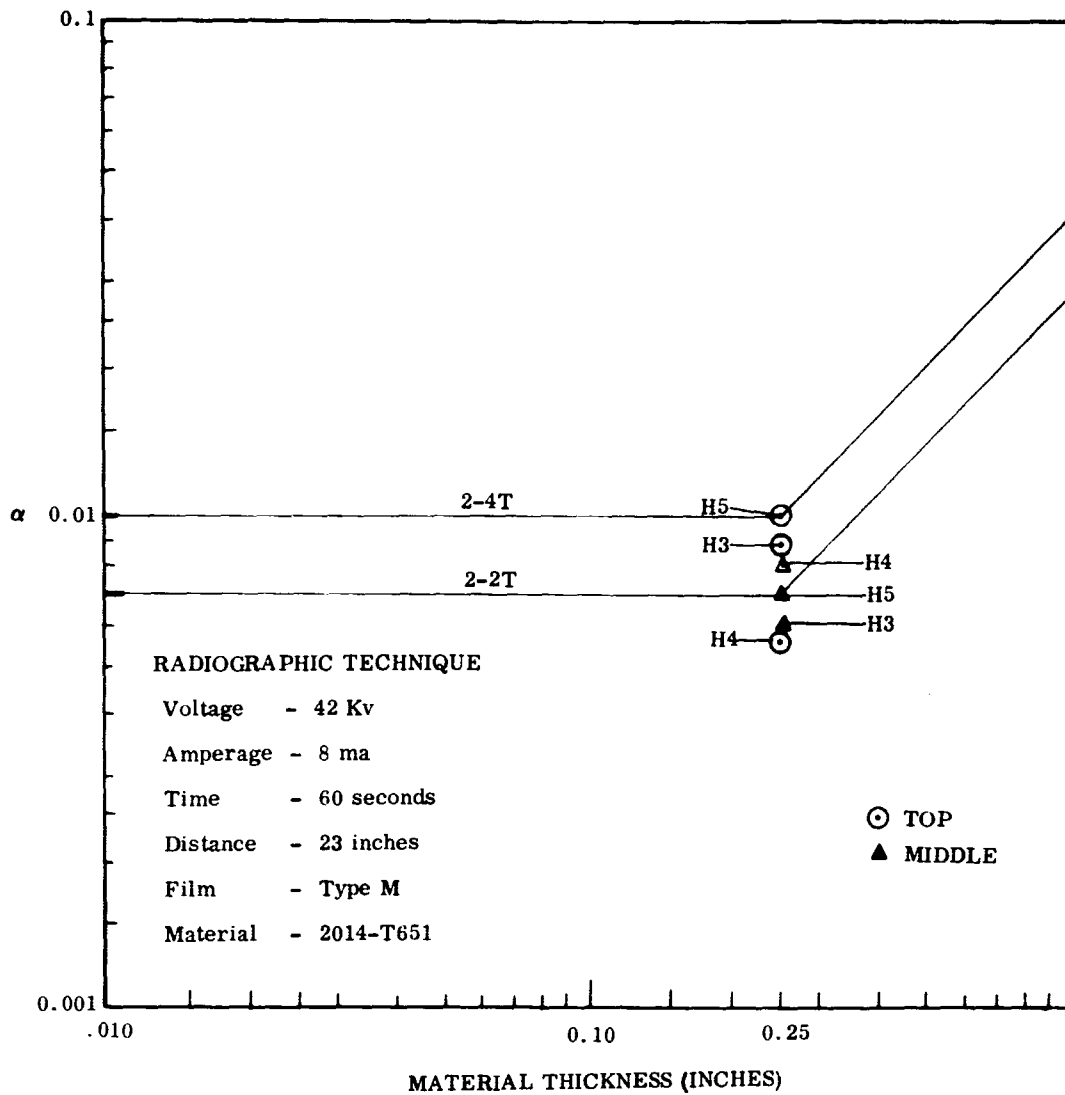


Figure 15. Minimum α Observed in H5, H4 and H3 Penetrators Compared to Quality Levels Required by MIL-STD-453

4.3 TAPER SLIT PENETRATORS

The radiographs for the five tapered slit penetrators placed at an angle of 0, 5, 10, 15, and 20 degrees to the x-ray beam are presented on pages A-17 through A-41 in the Appendix. The film density measurements obtained on each radiograph are shown in Table 9 and the location and number of readings taken were identical to those obtained on the graduated hole penetrators. Film density values ranged from 2.28 to 2.50 and indicated little or no difference in density values with respect to penetrator location or angle of the x-ray beam.

Table 9. Film Density⁽¹⁾ Measurements of Radiographs
for Slit Type Penetrameters

Penetrameter Identification	Penetrameter Location ⁽²⁾	Film Density@X-ray Beam Angle				
		0°	5°	10°	15°	20°
C-1	T	2.34	2.34	2.35	2.32	2.28
	M	2.40	2.34	2.40	2.32	2.30
C-2	T	2.36	2.32	2.40	2.34	2.30
	M	2.34	2.35	2.38	2.32	2.30
C-3	T	2.35	2.34	2.38	2.32	2.36
	M	2.42	2.36	2.39	2.30	2.36
C-4	T	2.36	2.37	2.42	2.40	2.32
	M	2.42	2.37	2.44	2.36	2.32
C-5	T	2.42	2.44	2.50	2.36	2.38
	M	2.42	2.42	2.50	2.42	2.40

(1) Average of three readings taken on the upper part of the plate between the penetrameter and Pb marking strip.

(2) T = Top
M = Middle

The minimum slit widths detectable in all thicknesses of penetrameters when placed on the top or in the middle of the test block and radiographed with the tapered slits at an angle of 0, 5, 10, 15, and 20 degrees to the x-ray beam are presented in Tables 10 through 14. The minimum, maximum, and average slit lengths shown in these tables represent only values which can be directly identified with the vanishing point of the tapered slit and assumes that the maximum slit width is located at the edge of the test block. Therefore, the average slit length as identified in these tables truly represents a specific location along the tapered slit which can be readily convertible to a minimum detectable slit width from Table 2. For example, in Table 10 the average slit length or vanishing point was 2.50 in. for the C-5 penetrameter placed on top of the test block. From Table 2, the slit width at 2.50 in., or at location number 10 is 0.9 mils. To obtain the slit width for a length falling between the one-quarter inch marks, interpolation was used.

Table 10. Minimum Slit Width Detectable, X-ray Beam Parallel to Slits (Fixed Radiographic Technique)

I. D.	Penetrator Thickness ⁽¹⁾ In.	Top			Avg. Width ⁽³⁾ In.	Middle			Avg. Width ⁽³⁾ In.
		Min.	Length, In. ⁽²⁾ Max.	Avg.		Min.	Length, In. ⁽²⁾ Max.	Avg.	
C-5	0.005	2.41	2.63	2.50	0.0009	2.38	2.68	2.57	0.0008
C-4	0.004	2.14	2.47	2.24	0.0012	1.88	2.41	2.18	0.0013
C-3	0.003	1.18	2.13	1.66	0.0018	1.75	2.08	1.86	0.0016
C-2	0.002	1.58	1.85	1.75	0.0026	1.75	1.98	1.86	0.0025
C-1	0.001	-	-	0.03 ⁽⁴⁾	-	-	-	0.02 ⁽⁴⁾	-

(1) Thickness equivalent to slit depth

(2) As measured from the edge of the test block to the vanishing point of the slit. Except as noted, values represent the average of 5 readings taken by 5 observers.

(3) Values obtained or derived from Table 2 for slit width measurements.

(4) One out of five observers reported this "slit" length which falls between the edge of the test block and the penetrator edge (see Figure 11).

Table 11. Maximum Slit Widths Detectable, X-ray Beam Angle 5° to Slits (Fixed Radiographic Technique)

I. D.	Penetrator Thickness (1) In.	Top			Avg. Width(3) In.	Middle			Avg. Width(3) In.
		Min.	Length, In. (2) Max.	Avg.		Min.	Length, In. (2) Max.	Avg.	
C-5	0.005	2.22	2.63	2.53	0.0008	2.39	2.75	2.58	0.0007
C-4	0.004	2.00	2.38	2.20	0.0013	2.03	2.36	2.22	0.0013
C-3	0.003	1.42	2.20	1.73	0.0017	1.38	1.88	1.62	0.0019
C-2	0.002	1.38	1.84	1.56	0.0029	1.31	2.21	1.75	0.0026
C-1	0.001	-	-	0.02 ⁽⁴⁾	-	-	-	0.01 ⁽⁴⁾	-

(1) Thickness equivalent to slit depth

(2) As measured from the edge of the test block to the vanishing point of the slit. Except as noted, values represent the average of 5 readings taken by 5 observers.

(3) Values obtained or derived from Table 2 for slit width measurements.

(4) One out of five observers reported this "slit" length which falls between the edge of the test block and the penetrometer edge (see Figure 11).

Table 12. Minimum Slit Widths Detectable, X-ray Beam Angle 10° to Slits (Fixed Radiographic Technique)

I. D.	Penetrator Thickness ⁽¹⁾ In.	Top			Avg. Width ⁽³⁾ In.	Middle			Avg. Width ⁽³⁾ In.
		Min.	Length, In. ⁽²⁾ Max.	Avg.		Min.	Length, In. ⁽²⁾ Max.	Avg.	
C-5	0.005	2.38	2.62	2.50	0.0009	2.30	2.62	2.47	0.0010
C-4	0.004	1.81	2.34	2.08	0.0015	1.80	2.36	2.20	0.0013
C-3	0.003	1.30	1.85	1.63	0.0018	1.28	1.64	1.47	0.0021
C-2	0.002	1.33	2.00	1.67	0.0027	1.04	1.88	1.59	0.0029
C-1	0.001	-	-	-	-	-	-	0.03 ⁽⁴⁾	-

(1) Thickness equivalent to slit depth.

(2) As measured from the edge of the test block to the vanishing point of the slit. Except as noted, values represent the average of 5 readings taken by 5 observers.

(3) Values obtained or derived from Table 2 for slit width measurements.

(4) One out of five observers reported this "slit" length which falls between the edge of the test block and the penetrator edge (see Figure 11).

Table 13. Minimum Slit Widths Detectable, X-ray Beam Angle 15° to Slits (Fixed Radiographic Technique)

I. D.	Penetrimeter Thickness(1) In.	Top			Avg. Width(3) In.	Middle			Avg. Width(3) In.
		Min.	Length, In.(2) Max.	Avg.		Min.	Length, In.(2) M&A.	Avg.	
C-5	0.005	2.19	2.55	2.35	0.0012	2.13	2.39	2.30	0.0013
C-4	0.004	1.76	2.13	1.93	0.0017	1.78	1.98	1.84	0.0019
C-3	0.003	1.08	1.28	1.13	0.0025	0.75	1.58	1.20	0.0025
C-2	0.002	0.63	1.33	0.88	0.0041	1.35	1.83	1.59	0.0029
C-1	0.001	-	-	-	-	-	-	0.02 ⁽⁴⁾	-

(1) Thickness equivalent to slit depth

(2) As measured from the edge of the test block to the vanishing point of the slit. Except as noted, values represent the average of 5 readings taken by 5 observers.

(3) Values obtained or derived from Table 2 for slit width measurements.

(4) One out of five observers reported this "slit" length which falls between the edge of the test block and the penetrometer edge (see Figure 11).

Table 14. Minimum Slit Widths Detectable, X-ray Beam Angle 20° to Slits (Fixed Radiographic Technique)

I. D.	Penetrator Thickness ⁽¹⁾ In.	Top			Avg. Width ⁽³⁾ In.	Middle			Avg. Width ⁽³⁾ In.
		Min.	Length, In. (2) Max.	Avg.		Min.	Length, In. (2) Max.	Avg.	
C-5	0.005	2.00	3.00	2.30	0.0013	2.03	2.75	2.33	0.0012
C-4	0.004	1.78	2.89	2.09	0.0015	1.50	1.80	1.66	0.0024
C-3	0.003	0.53	1.80	0.97	0.0028	1.05	1.83	1.32	0.0023
C-2	0.002	0.78	1.38	1.08	0.0038	1.08	1.85	1.35	0.0033
C-1	0.001	-	-	-	-	-	-	-	-

(1) Thickness equivalent to slit depth.

(2) As measured from the edge of the test block to the vanishing point of the slit. All values represent the average of 5 readings taken by 5 observers.

(3) Values obtained or derived from Table 2 for slit width measurements.

The minimum slit dimensions detectable for all test variables investigated and under the fixed radiographic technique are shown in Figures 16 through 20; in each case slit depth or penetrameter thickness is plotted as a function of slit width (log-log). Data points represent an average of five readings and a straight line drawn down through these data points resulted in an average slope varying between -0.70 and -0.81 .

Table 15 provides a summary of the maximum detectable slit lengths observed by five analysts for each thickness, penetrameter location, and x-ray beam angle. Values shown represent the distance measured between maximum slit width opening at the penetrameter edge to the vanishing point of the slit and are included as a reference to identify and compare major differences between the test variables. Table 16 summarizes the slit dimensions detectable for the fixed radiographic technique at x-ray beam angles of 0, 5, 10, 15, and 20 degrees and further tabulates the differences noted in resolving slit length and width as a function of penetrameter location and x-ray beam angles.

4.4 X-RAY BEAM UNIFORMITY

A contour map prepared to evaluate the uniformity of the x-ray beam under test conditions similar to those used in this test program is shown in Figure 21. The position of the penetrameter test blocks during radiography is superimposed upon the map to identify the area over which the density measurements were taken. The results show only a minor variation in density occurs over the entire area selected to obtain density readings for this test program. The average difference in diffuse transmission density numbers did not exceed ± 0.05 .

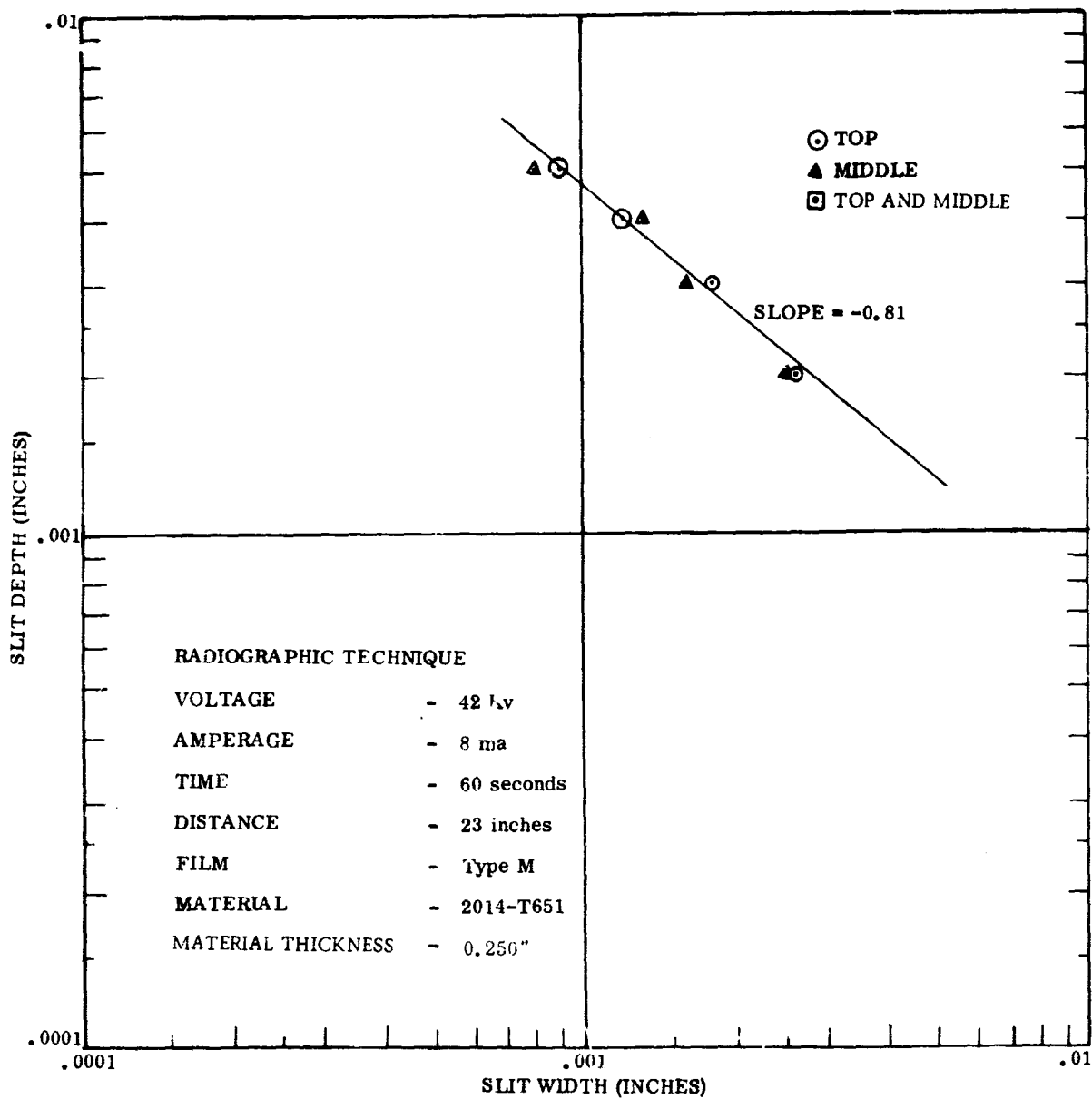


Figure 16. Minimum slit dimension detectable for a fixed radiographic technique - slit parallel (0°) to x-ray beam.

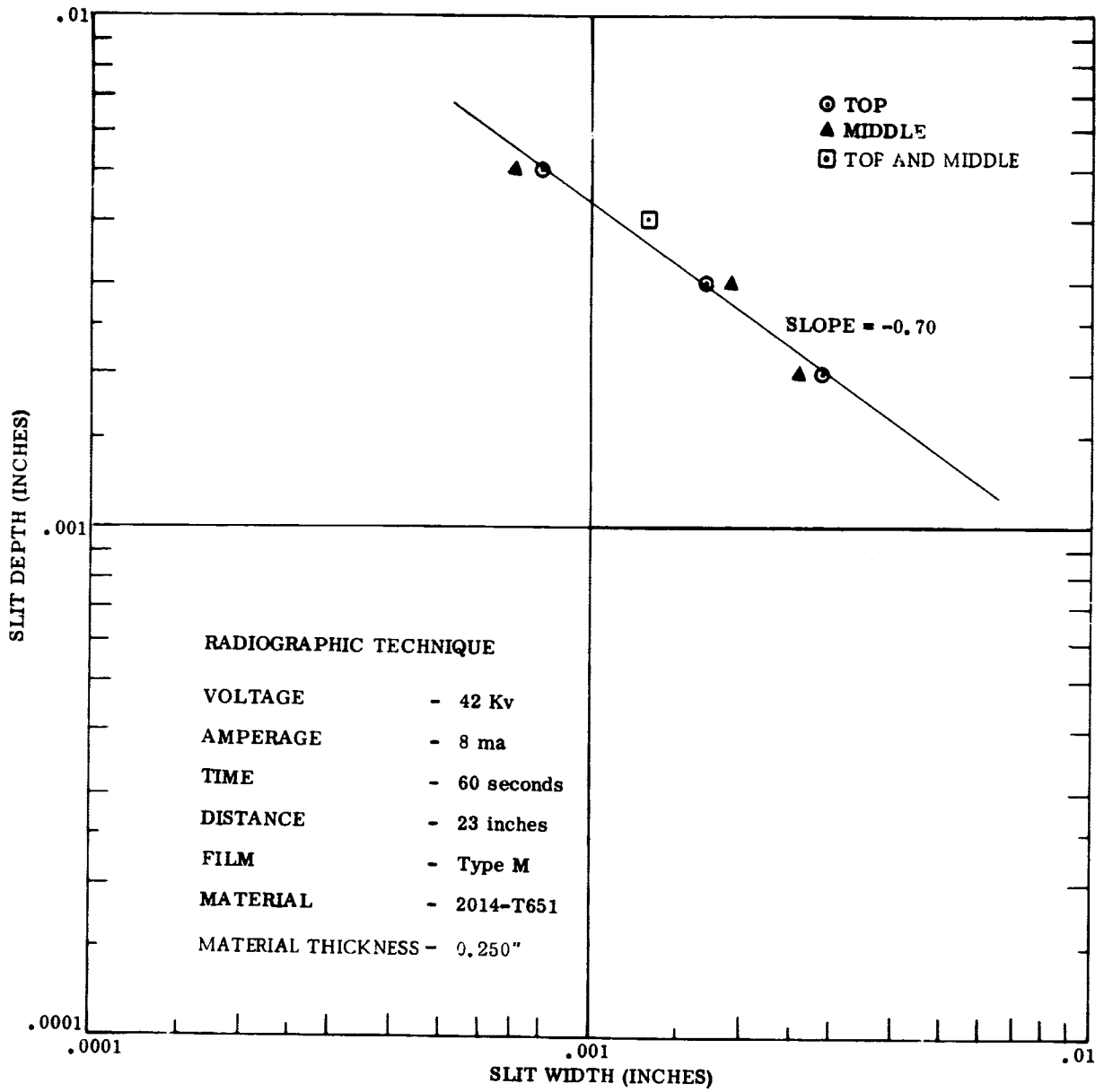


Figure 17. Minimum slit dimension detectable for a fixed radiographic technique - slit 5° to x-ray beam.

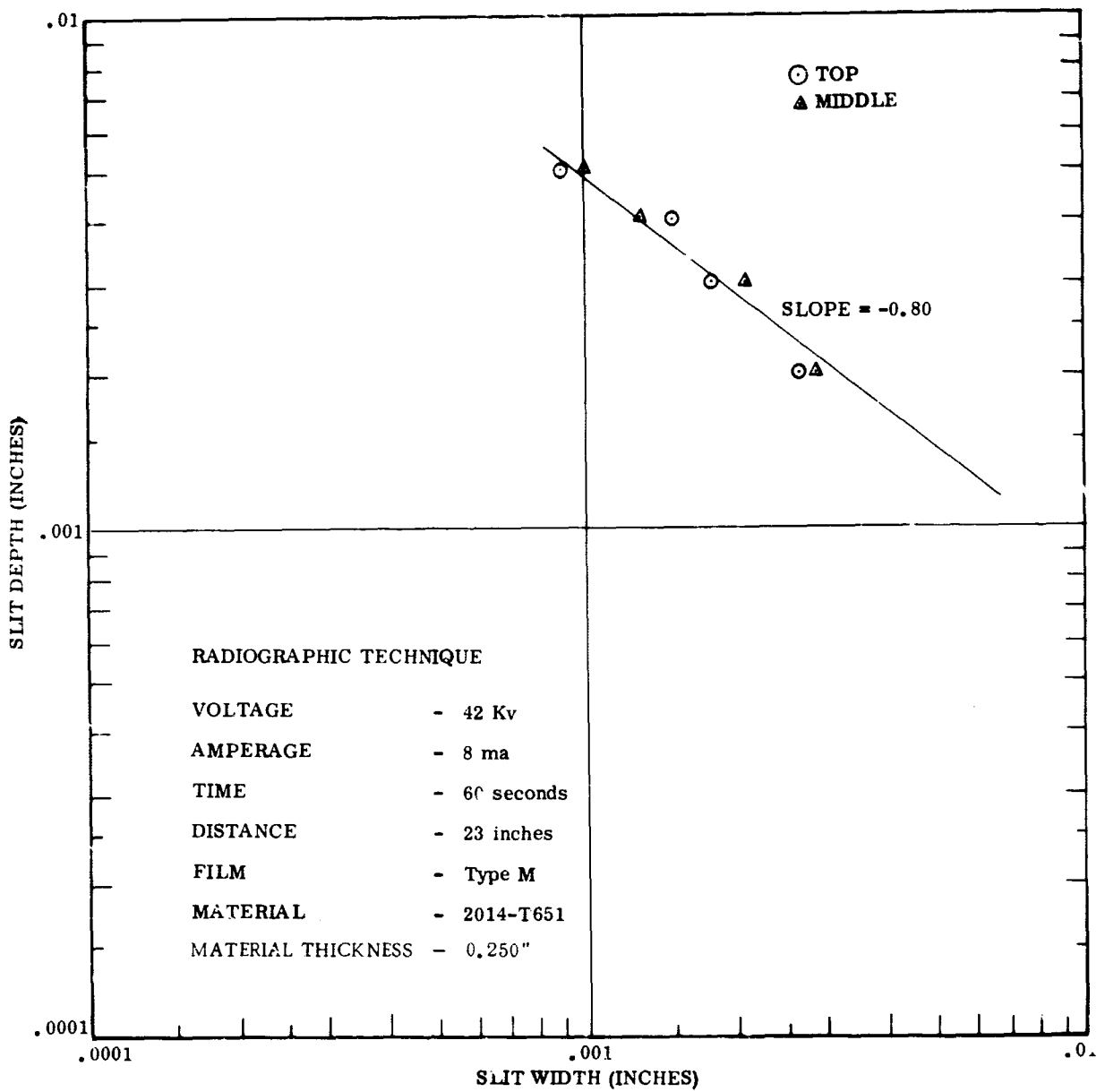


Figure 18. Minimum slit dimension detectable for a fixed radiographic technique - slit 10° to x-ray beam.

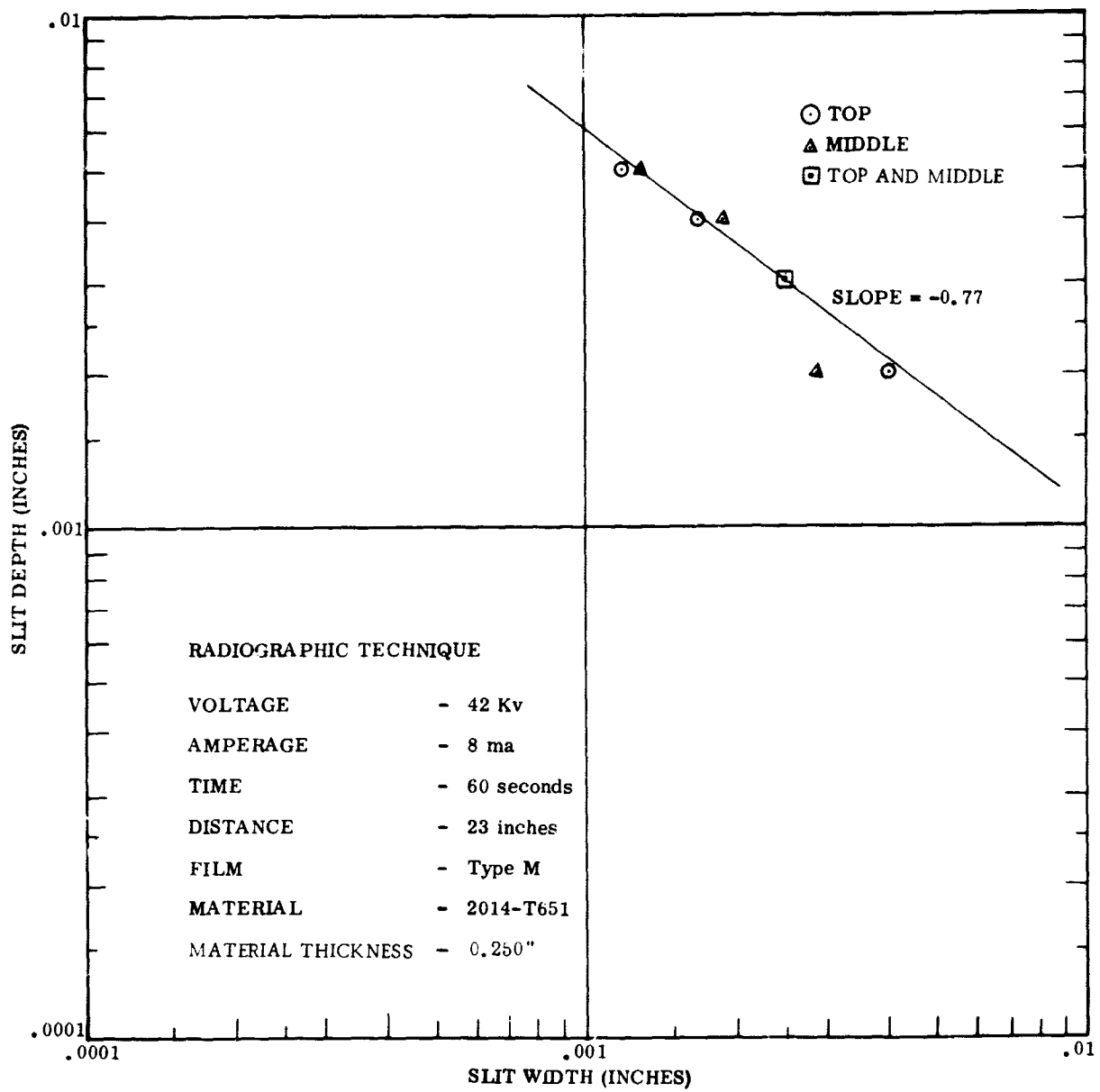


Figure 19. Minimum slit dimension detectable for a fixed radiographic technique - slit 15° to x-ray beam.

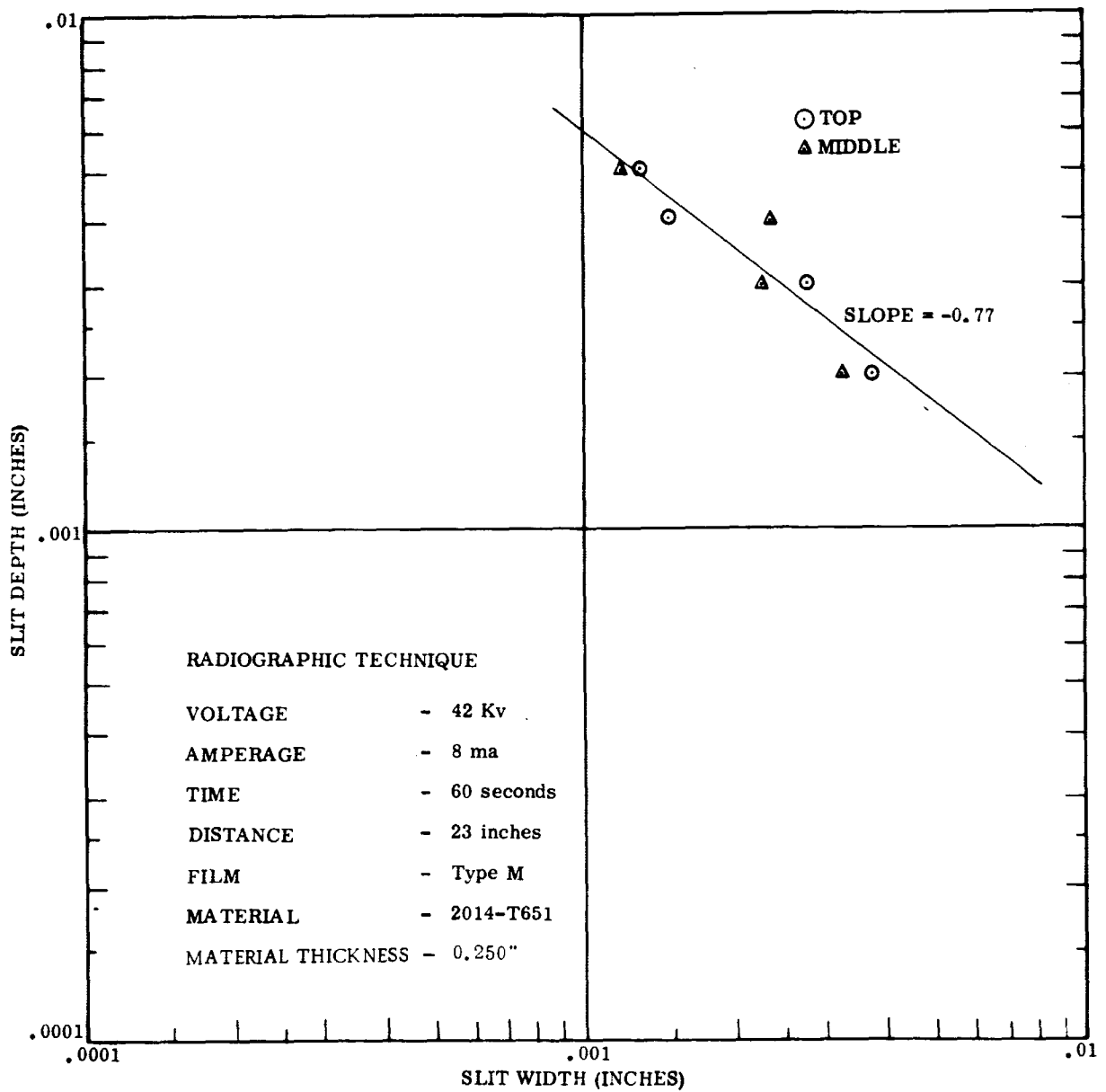


Figure 20. Minimum slit dimension detectable for a fixed radiographic technique - slit 20° to x-ray beam.

Table 15. Maximum Slit Lengths Detectable for a Fixed Radiographic Technique

Penetrator Thickness, Inches	Slit Length in Inches (1)(2)														
	0°			5°			10°			15°			20°		
	T (3)	M		T	M		T	M		T	M		T	M	
C-5 0.005	2.36	2.43		2.39	2.44		2.36	2.33		2.21	2.16		2.16	2.19	
C-4 0.004	2.12	2.06		2.08	2.10		1.96	2.08		1.81	1.72		1.97	1.54	
C-3 0.003	1.57	1.77		1.64	1.53		1.54	1.38		1.04	1.11		0.88	1.23	
C-2 0.002	1.60	1.71		1.41	1.60		1.52	1.44		0.73	1.44		0.93	1.20	
C-1 ⁽⁴⁾ 0.001	—	—		—	—		—	—		—	—		—	—	

(1) All values are averages of 5 measurements taken by 5 observers.

(2) Distance between the "O" location at penetrator edge to vanishing point of slit (see Figure 11).

(3) Location of penetrator at T and M refers to TOP and MIDDLE, respectively.

(4) Slit was not observed in radiographs for the C-1 penetrators.

Table 16. Summary of Slit Dimensions Detectable for a Fixed Radiographic Technique

Slit Depth Inches	Beam Angle Degrees	Minimum Width (1) (5) Inches	$T_w - M_w$ (2) (5) Inches	T or M Δl Max. (2) (4) (5) Inches
0.005	0	0.0008	+0.0001	0.30
	5	0.0007	+0.0001	0.41
	10	0.0009	-0.0001	0.32
	15	0.0012	-0.0001	0.36
	20	0.0012	+0.0001	1.00
0.004	0	0.0012	-0.0001	0.53
	5	0.0013	0.0000	0.38
	10	0.0013	+0.0002	0.56
	15	0.0017	-0.0002	0.37
	20	0.0015	-0.0009	1.11
0.003	0	0.0016	+0.0002	0.95
	5	0.0017	-0.0002	0.78
	10	0.0018	-0.0003	0.55
	15	0.0025	0.0000	0.83
	20	0.0023	+0.0005	1.27
0.002	0	0.0025	+0.0001	0.27
	5	0.0026	+0.0003	0.90
	10	0.0027	-0.0002	0.84
	15	0.0029	+0.0012	0.70
	20	0.0033	+0.0005	0.77
0.001	0	(3)	-	-
	5	(3)	-	-
	10	(3)	-	-
	15	(3)	-	-
	20	(3)	-	-

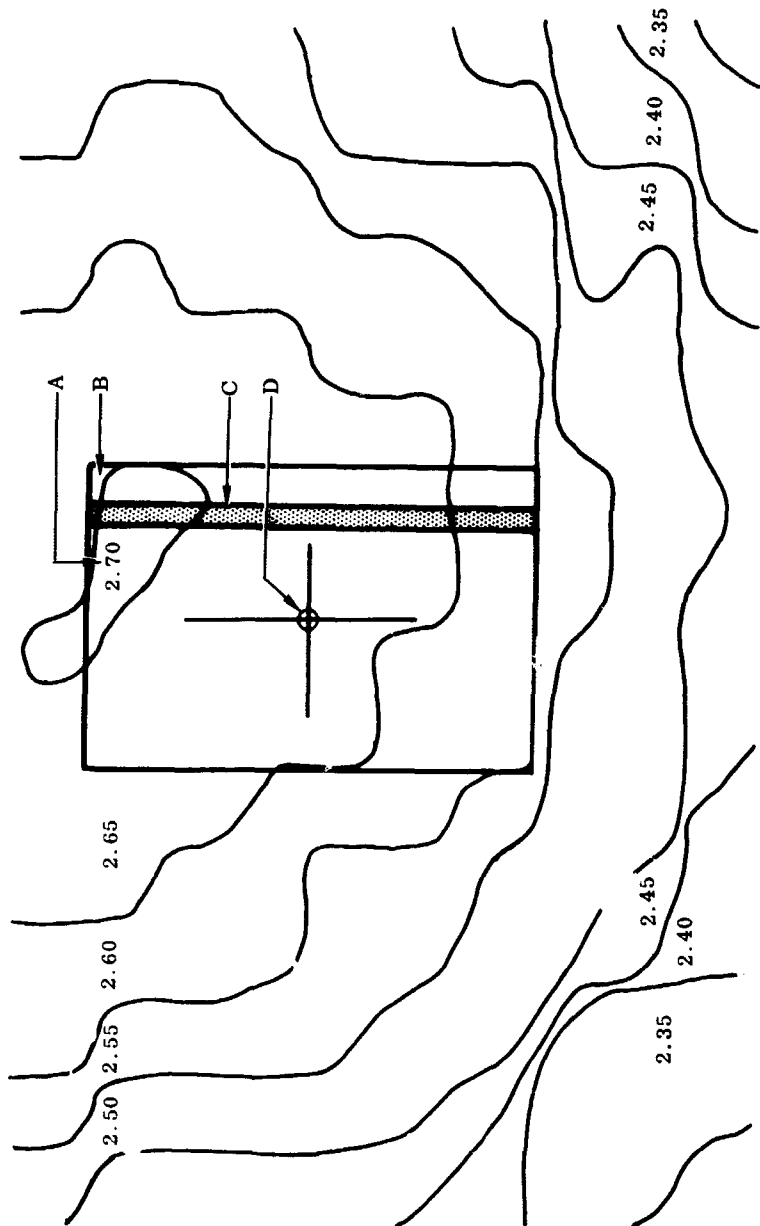
(1) Average of five readings.

(2) T = Top; M = Middle; w = Slit Width; l = Slit Length.

(3) Slit was not detectable by any observer.

(4) To estimate change in slit width, multiply Δl value by 0.002.

(5) Information from Tables 10 through 14.



TEST CONDITIONS:

- | | |
|--------------|---------------------------------|
| 1. Voltage | 42Kv |
| 2. Amperage | 8 ma |
| 3. TFD | 23 inches |
| 4. FS | 1.5 mm |
| 5. Film | Type M-14"x17" |
| 6. Filter | 1/4" - 2014-T651 Aluminum Alloy |
| 7. Developed | 5 Minutes @ 68 ± 1° F |

- A = Diffuse Transmission Density Number
- B = Penetrator Test Block
- C = Density Reading Area on Radiographic Film
- D = Geometric Centerline of X-Ray Beam

Figure 21. X-ray Beam Uniformity - OEG 50 AW Tube

SECTION 5
CONCLUSIONS

Based upon the experimental test data obtained during this investigation and the information contained within this report, the following conclusions are made:

- a. It has been demonstrated that penetrameters designed to simulate crack depths between 0.001 in. and 0.005 in. can be prepared by employing tapered slits and special fabrication techniques, and that equally thin hole-type penetrameters with straight, clean-bored hole diameters equal to $T/3$ are now within the current state of the art.
- b. Based on the average readings of the five analysts, the minimum slit dimensions detectable in the one-quarter inch aluminum welds for the fixed radiographic technique, and with slits parallel to the x-ray beam, were as follows:
 1. 0.0008 in. x 0.005 in.
 2. 0.0012 in. x 0.004 in.
 3. 0.0016 in. x 0.003 in.
 4. 0.0025 in. x 0.002 in.
- c. Factors controlling the minimum detectable slit widths were, in order of importance:
 1. Density variations within the weld area
 2. Visual acuity of the analysts
 3. Slit depth
 4. X-ray beam angle
 5. Penetrameter location
- d. Based upon the average values determined for resolvable slit dimensions, the following relationships exist:
 1. Minimum detectable slit width increased as the slit depth decreased from 0.005 in. to 0.001 in. and the x-ray beam angle increased from 0° to 20° .
 2. For any given slit depth between 0.002 in. and 0.005 in., the minimum detectable slit width was not significantly influenced by an x-ray beam angle between 0° and 10° .
 3. With few exceptions, the location of the penetrameter within the test block had little or no significant effect on the resolution of slit images.

- e. Based upon a comparison of the minimum and maximum values obtained for slit lengths, the vanishing point of the tapered slit image varied considerably from analyst to analyst and is believed to be the largest single factor contributing to the scatter in the test data. Slit length measurements were found to vary between 1/4 in. and 1 1/4 in. with the largest variation occurring in slit depths 0.003 in. or less and at an x-ray beam angle greater than 15°. The differences in slit length measurements were more consistent and did not exceed 1/2 in. for slit depths of 0.005 in. and 0.004 in. and at x-ray beam angles of 0°, 5°, 10° and 15°.
- f. When the minimum detectable slit widths were plotted as a function of slit depth, the slope of the straight line drawn through all data points varied between -0.70 and -0.81 indicating that unsharpness was a significant factor in the resolution of the slit image. This was particularly evident for slit depths less than 0.004 in. and at x-ray beam angles greater than 10°. For slit depths of 0.004 in. and 0.005 in. and at x-ray beam angles of 0°, 5°, and 10°, the slope of the line drawn through these data points approaches the ideal value of -0.50, where the unsharpness factor is negligible.
- g. The average analyst was capable of resolving at least one or more round hole image in 0.003, 0.004, and 0.005-in. thick graduated hole-type penetrameters located in the weld. The minimum hole diameter perceptible to all analysts was the 2T hole in the 0.004-in. thick penetrameter. Based upon the minimum alpha values observed by the average analyst, the hole visibility in 0.003, 0.004, and 0.005-in. thicknesses was equivalent to a radiographic quality level of 2-4T or less and a radiographic quality level of 2-2T was achieved more frequently when the penetrameter was located in the middle of the test plates. It is believed that density variations within the weld area were a major factor in reducing the visibility of the hole image by the average film reader.
- h. The dark linear indications found during the radiographic examination of these simulated production welds were attributed to the diffraction and/or reflection effect resulting from the preferred orientation of large dendritic grains. It is believed that radiographic images of tight cracks or microfissures oriented parallel to the dendritic grains would be completely masked by these indications, particularly if the defect dimension were similar to those investigated in this test program. Therefore, such cracks would be unresolvable under the most refined technique and by the most experienced film interpreters.
- i. The double film technique was not considered a reliable means of obtaining a duplicate set of standard radiographs under the test conditions established for this program because the resolution of hole images on certain back films was significantly reduced. The 2T hole was not visible in 40 percent of the back film when a MIL-STD-453 aluminum penetrameter, placed outside the weld area, was sandwiched between the test plates. With this exception, however, a radiographic quality level of 2-2T was readily obtained for the fixed radiographic technique regardless of film or penetrameter location and within the density range of 2.1 to 2.4.

- j. Fatigue cracks were produced in 0.002, 0.003, 0.004, and 0.005-in. aluminum foil using the single edge notched (SEN) specimen configuration. However, resultant fractured edges did not meet the test requirements for simulating the flat or brittle-type edges of a natural crack because the low loads required to produce this type of crack were not within the capabilities of the fatigue testing equipment. This method of simulating a natural crack with flat edges was discarded in favor of machined tapered slits.

SECTION 6

RECOMMENDATIONS

It has been demonstrated that the tapered slit-type penetrameters specially designed to simulate crack depths between 0.001 in. and 0.005 in. can be prepared employing special fabrication techniques and that equally thin hole-type penetrameters with straight, clean-bored hole diameters equal to T/3 are now within the current state of the art. Furthermore, the test results show that these slit-type penetrameters can be used as standards capable of defining, quantitatively, the minimum detectable crack dimensions in thin aluminum plate welds for a specific radiographic technique.

It is recommended, therefore, that the application of these special penetrameters be extended to include experiments designed to:

- a. Develop improved radiographic techniques suitable for inspecting production welds in material thicknesses one-quarter inch and less utilizing the capability of the newly developed penetrameters matched with the latest development in radiographic equipment and film. This is particularly applicable to present and future high strength, lightweight aerospace hardware designed from thin gage high strength, weldable grades of aluminum, titanium, and steel; e.g., cryogenic liquid propellant tankage systems.
- b. Evaluate and compare the suitability of hole, slit, and wire penetrameters as technique indicators for measuring the radiographic sensitivity of relatively thin gage materials most commonly selected for flight vehicle structures employing cryogenic fuels and oxidizers. Wire penetrameters in particular may be the most suitable technique indicator for thin gage materials for optimizing radiographic techniques and defining the threshold capabilities of cracks. Therefore, their capabilities should be examined in depth.
- c. Evaluate and compare those parameters which control the resolution of images and affect the radiographic quality levels in 2014, 2219, and 2021 aluminum alloy weldments. Emphasis should be placed on defining the optimum radiographic technique capable of providing maximum structural reliability consistent with production requirements.
- d. Investigate and evaluate the application of the automatic recording microdensitometer as a production tool for identifying and measuring radiographic images. This technique will provide objective quantitative measurements of film densities and gradients over very small film areas. Therefore, a comparison of the threshold detection capabilities of this equipment should be made with respect to those obtainable by human observation.

SECTION 7

REFERENCES

1. Eddy Current Probe Measures Size of Cracks in Nonmetallic Materials, NASA Tech Brief 67-10645, December 1967.
2. Criscuolo, E. L., "Slit Detection by Radiography," Materials Evaluation, Journal of ASNT, Vol. XXIV, No. 4, Pages 201-205.
3. Criscuolo, E. L., Equivalence of Penetrameter Systems, U. S. Naval Ordnance Laboratory Report NOLTR 62-49, July 1962
4. Criscuolo, E. L. and Polansky, D., "The Application of Radiographic Specifications," Nondestructive Testing, Journal of ASNT, Vol. XX, No. 2, Pages 114-118.
5. Splettstosser, H. R., "The Visibility of Detail Obtainable with Industrial X-ray Film," Materials Evaluation, Journal of ASNT, Vol. XXV, No. 11, Pages 245-253.
6. Baker, J. M., and Vannier, R. K., "Influence of Technique Variables on Radiographic Quality Levels in the X-ray Examination of Titanium," presented at the ASNT 1968 Spring Symposium on NDT of Welds and Materials Joining at Los Angeles, California, March 1968.
7. Rummel, W. D., and Gregory, B. E., "Ghost Lack of Fusion in Aluminum Alloy Welds," Material Evaluation, December 1965, Pages 586-588.
8. Tucker, M. S., and Larssen, P. A., "Markings in Radiographs of 2014 Aluminum Alloy Gas Tungsten-Arc Welds," Welding Journal, Vol. 47, No. 5, Pages 223s-225s, May 1968.
9. "Mechanical Microdrilling Outperforms Even the Laser," Product Engineering, Vol. 38, No. 26, December 18, 1967, Page 96.